(12)

WT-76(EX)
EXTRACTED VERSION

OPERATION GREENHOUSE

Scientific Director's Report of Atomic Weapon Tests at Eniwetok, 1951

Annex 1.2, Delayed Gamma-ray Measurements
Part 1, Gamma-ray Spectrum Measurements (Abridged)

H. F. Gibson
W. Miller
J. W. Motz
J. C. Smeltzer
H. O. Wyckoff
Radiation Physics Laboratory
National Bureau of Standards
Washington, DC

April 1952

NOTICE:
This is an extract of WT-76, Operation GREENHOUSE, Annex 1.2, Part 1.

Extracted version prepared for
Director
DEFENSE NUCLEAR AGENCY
Washington, DC 20305-1000

1 September 1985

Destroy this report when it is no longer needed. Do not return to sender.

PLEASE NOTIFY THE DEFENSE NUCLEAR AGENCY, ATTN: STTI, WASHINGTON, DC 20305-1000, IF YOUR ADDRESS IS INCORRECT, IF YOU WISH IT DELETED FROM THE DISTRIBUTION LIST, OR IF THE ADDRESSEE IS NO LONGER EMPLOYED BY YOUR ORGANIZATION.

UNCLASSIFIED
SECURITY CLASSIFICATION OF THIS PAGE

REPORT DOCUMENTATION PAGE

Form Approved OMB No. 0704-0188 Exp. Date: Jun 30, 1986

1a. REPORT SECURITY CLASSIFICATION: UNCLASSIFIED	1b. RESTRICTIVE MARKINGS
2a. SECURITY CLASSIFICATION AUTHORITY: N/A since Unclassified	3. DISTRIBUTION/AVAILABILITY OF REPORT: Approved for public release; distribution is unlimited.
2b. DECLASSIFICATION/DOWNGRADING SCHEDULE: N/A since Unclassified	
4. PERFORMING ORGANIZATION REPORT NUMBER(S)	5. MONITORING ORGANIZATION REPORT NUMBER(S): WT-76(EX)
6a. NAME OF PERFORMING ORGANIZATION: Radiation Physics Laboratory, National Bureau of Standards; 6b. OFFICE SYMBOL (If applicable)	7a. NAME OF MONITORING ORGANIZATION: Defense Atomic Support Agency
6c. ADDRESS (City, State, and ZIP Code): Washington, DC	7b. ADDRESS (City, State, and ZIP Code): Washington, DC
8a. NAME OF FUNDING/SPONSORING ORGANIZATION; 8b. OFFICE SYMBOL (If applicable)	9. PROCUREMENT INSTRUMENT IDENTIFICATION NUMBER
8c. ADDRESS (City, State, and ZIP Code)	10. SOURCE OF FUNDING NUMBERS: PROGRAM ELEMENT NO; PROJECT NO; TASK NO.; WORK UNIT ACCESSION NO

11. TITLE (Include Security Classification) OPERATION GREENHOUSE, Scientific Director's Report of Atomic Weapon Tests at Eniwetok, 1951; Annex 1.2, Delayed Gamma-ray Measurements; Part I, Gamma-ray Spectrum Measurements (Abridged), Extracted Version

12. PERSONAL AUTHOR(S): Gibson, H.F.; Miller, W.; Motz, J.W.; Smeltzer, J.C.; Wyckoff, H.O.

13a. TYPE OF REPORT	13b. TIME COVERED	14. DATE OF REPORT (Year, Month, Day)	15. PAGE COUNT
Scientific Director's	FROM _____ TO _____	520400	62

16. SUPPLEMENTARY NOTATION: This report has had sensitive military information removed in order to provide an unclassified version for unlimited distribution. The work was performed by the Defense Nuclear Agency in support of the DoD Nuclear Test Personnel Review Program.

17. COSATI CODES			18. SUBJECT TERMS (Continue on reverse if necessary and identify by block number)
FIELD	GROUP	SUB-GROUP	Greenhouse; Gamma-ray Measurements; Spectrometers; Gamma-ray Spectra
18	3		
20	8		

19. ABSTRACT (Continue on reverse if necessary and identify by block number)

The measurement of bomb efficiencies from the number of gamma-rays requires fundamentally two separate experiments. The average number of gamma-rays emitted from the fission fragments (delayed gamma-rays) per fission must be determined. This experiment can be carried out in the laboratory. A second experiment, the absolute determination of the number of gamma-rays from the bomb was also attempted. Because gamma-rays are not directly observable but are measurable only through their secondary effects, and because the probability of occurrence of the secondary effects depends upon the gamma-ray energy, it is not usually possible to count directly the number of gamma-rays in a heterochromatic spectrum. A spectral distribution must be first obtained from which the actual total number of gamma-rays may be computed.

The planning for the experiment and the spectral distribution of collimated gamma-rays determined from the Greenhouse tests on two shots are discussed in detail in this volume. A discussion of measurement of build-up factor which is needed to estimate the effect of collimation is also given.

20. DISTRIBUTION/AVAILABILITY OF ABSTRACT	21. ABSTRACT SECURITY CLASSIFICATION	
☒ UNCLASSIFIED/UNLIMITED ☐ SAME AS RPT ☐ DTIC USERS	UNCLASSIFIED	
22a. NAME OF RESPONSIBLE INDIVIDUAL: MARK D. FLOHR	22b. TELEPHONE (Include Area Code): (202) 325-7559	22c. OFFICE SYMBOL: DNA/ISCM

DD FORM 1473, 84 MAR — 83 APR edition may be used until exhausted. All other editions are obsolete.

SECURITY CLASSIFICATION OF THIS PAGE
UNCLASSIFIED

FOREWORD

Classified material has been removed in order to make the information available on an unclassified, open publication basis, to any interested parties. The effort to declassify this report has been accomplished specifically to support the Department of Defense Nuclear Test Personnel Review (NTPR) Program. The objective is to facilitate studies of the low levels of radiation received by some individuals during the atmospheric nuclear test program by making as much information as possible available to all interested parties.

The material which has been deleted is either currently classified as Restricted Data or Formerly Restricted Data under the provisions of the Atomic Energy Act of 1954 (as amended), or is National Security Information, or has been determined to be critical military information which could reveal system or equipment vulnerabilities and is, therefore, not appropriate for open publication.

The Defense Nuclear Agency (DNA) believes that though all classified material has been deleted, the report accurately portrays the contents of the original. DNA also believes that the deleted material is of little or no significance to studies into the amounts, or types, of radiation received by any individuals during the atmospheric nuclear test program.

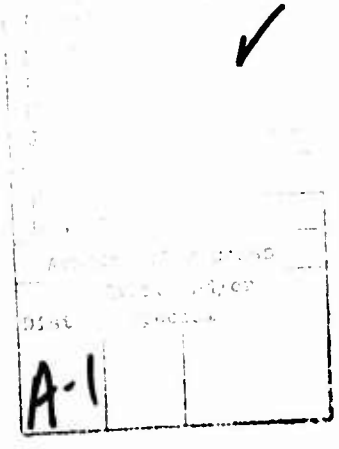

Scientific Director's Report of Atomic Weapon Tests at Eniwetok, 1951

Annex 1.2

Delayed Gamma-ray Measurements

Part I—Gamma-ray Spectrum Measurements

Pages ii,iii,iv deleted.

DELAYED GAMMA-RAY MEASUREMENTS

Part I—Gamma-ray Spectrum Measurements (Abridged)

by

H. F. GIBSON
WILLIAM MILLER
J. W. MOTZ
J. C. SMELTZER
H. O. WYCKOFF

Approved by: FREDERICK REINES
Director, Program 1

Approved by: ALVIN C. GRAVES
Scientific Director

Radiation Physics Laboratory
National Bureau of Standards
Washington, D. C.

April 1952

Page vi blank.

Acknowledgments

The authors should like to express their appreciation to the J-7 group at Los Alamos, particularly Bob E. Watt, for many helpful suggestions. Dr. Watt also provided liaison between Los Alamos and the National Bureau of Standards.

Others who made significant contributions to the project both at the National Bureau of Standards and in the field are as follows:

Maj John P. Grant, USAF, and Allen A. Shoup — magnetic recorder; Frederick Kirn — spectrometer design and calibration; Carmen Cialella, Solomon Levine, Morris Kenny, Henry Kistner, and Stanley Matchett — spectrometer development and installation; and Sgts Warren Frain, Rayln E. Leatherby, Emery R. Lundy, and Frank J. Reilly — electronic development and installation.

Page viii blank.

CONTENTS

CONTENTS (Continued)

ILLUSTRATIONS

CHAPTER 2 SPECTROMETER DESIGN

CHAPTER 3 RESULTS

TABLES

Chapter 1

Introduction

1.1 PURPOSE

Several measurements of the gamma-ray spectrum have been made during the previous atomic bomb tests by means of absorption experiments. These measurements served as only a rough index of the spectral composition.[1] It was pointed out, however, during the planning of the Greenhouse tests that an absolute determination of the spectrum could be used to determine the efficiency* of the bomb. It was suggested that such a method might even be less costly and more accurate than the radiochemical methods previously used. The spectrum measurements might also provide a good check of the radiochemical methods during the present tests.

The measurement of bomb efficiencies from the number of gamma rays requires fundamentally two separate experiments. The average number of gamma rays emitted from the fission fragments (delayed gamma rays) per fission must be determined. This experiment can be carried out in the laboratory. The Los Alamos group under Bob Watt agreed to obtain this information. (A spectral and time distribution was also required here.) A second experiment, the absolute determination of the number of gamma rays from the bomb, will be attempted by the National Bureau of Standards.

Because gamma rays are not directly observable but are measurable only through their secondary effects, and because the probability of occurrence of the secondary effects depends upon the gamma-ray energy, it is not usually possible to count directly the number of gamma rays in a heterochromatic spectrum. A spectral distribution must first be obtained from which the actual total number of gamma rays may be computed. The planning for the experiment and the spectral distribution of collimated gamma rays determined from the Greenhouse tests on two shots will be discussed in detail in this volume. A discussion of a measurement of build-up factor which is needed to estimate the effect of collimation is given in reference 12.

* The efficiency is defined as the percentage of active material fissioning.

1.2 COMPTON SPECTROMETERS

The Compton effect has been used in both the cloud chamber and electron spectrometers to measure gamma-ray spectra. In the present experiment the cloud chamber is too slow to be considered. Electron spectrometers for measuring both beta and gamma radioactive sources have been used for many years. With this instrument it is possible to measure a spectrum to almost any desired accuracy, to determine background and pair-production correction, and to cover the desired energy range with adequate time resolution. Since it fits all the requirements for the present application, the Compton spectrometer was selected for use in measuring the gamma-ray spectrum on these tests. Details of the design and use of such an instrument will be included in the following chapters of this report and in reference 13.

1.3 DESIGN CRITERIA

Several factors, which are nearly independent of the type of measurement employed, may be used to limit the scope of this experiment.

They include (1) economic factors such as the number of measuring positions and the time of recording, (2) background knowledge of the spectrum obtained from previous tests, and (3) general information of gamma-ray phenomena.

1.3.1 Upper Energy Limit

On the Sandstone tests W. E. Ogle found gamma-induced threshold activities which indicated that some of the gamma rays from the bomb have energies[2] above 10 Mev. The activities were such that less than 1 per cent of the total spectral intensity could be assumed to be above this limit. For the present planning it was assumed that most of this 1 per cent resulted from gamma rays near 10 Mev.* The findings by Ogle and the above assumption served to set an upper limit of approximately 12 Mev for the present measurements.

1.3.2 Lower Energy Limit

The practical lower limit for the measured spectrum does not depend upon the lowest energy which can be readily measured. This limit is set by the air attenuation, the acceptable time of recording, and the permissible shadowing of more remote observation stations. Air attenuation between the observation station and the fission fragments is selective, i.e., the lower energies are attenuated more than the higher energies.

If the pressure and temperature of the air are known, it is possible to predict theoretically the radiation attenuation under narrow beam (good geometry) conditions. Two hundred meters of Eniwetok air will attenuate 5-Mev gamma rays to approximately 55 per cent; 0.5 Mev to 12 per cent; and 0.1 Mev to 2 per cent. These figures indicate the importance of placing the observation stations as near to the bomb as possible. On the other hand, near stations, and especially the equipment that they contain, cannot be expected to survive the blast; therefore the recording time is limited to the time from detonation of the bomb until the blast reaches the observation station. A station at 200 meters from the bomb is thus limited to approximately 25 msec of recording. After considering these two factors and the possible shadowing of other experiments by the final shelter design, a position was chosen for the near spectral measuring Station 54 at a radial distance of 610 ft from zero for each of the two shots. From the above considerations 0.5 Mev seemed to be an acceptable lower limit for the spectral measuring device.

In order to follow the spectrum to longer times than 25 msec, Station 57 was proposed at 2185 ft from zero for each of the two shots. At this location[4] 0.3 sec of recording time could be guaranteed. If the blast does not affect the measuring equipment, data may be obtained for even longer times. Data from Station 57 when compared with that from Station 54 will also provide a measure of the gamma-ray air scattering for the Greenhouse operations. The air scattering so determined may then be compared with that obtained by scaled experiments with radioactive sources[5] made in the laboratory. Because of the advantages of such a comparison, it was considered necessary to provide the same lower limit, 0.5 Mev, to the energy range of the spectrometers at Station 57.

1.3.3 Time Resolution

In addition to the delayed gamma rays whose number is to be determined, there are also prompt gamma rays accompanying the fission process. These prompt gamma rays are attenuated by the tamper, and so the number observed is a strong function of the bomb construction. Therefore a measurement of the prompt gamma rays does not offer a means of determining the bomb efficiency, but their presence may cause large errors in determinations based on the number of delayed gamma rays. For the present experiment the fissionable material will be so widely dispersed and the neutron flux will be so low that a negligible number of fissions would occur after 1 msec. (At 1 msec it is anticipated that the fission fragments will be distributed uniformly throughout a sphere having an approximate radius of 37 meters.) The present experiments are thus planned so that the first millisecond of recording can be eliminated.

The laboratory experiments,[6] Sandstone,[7] and the theory[8] indicate that the intensity should change only slowly, if at all, ($t^{-1.2}$) with time during the expected interval of the spectral

* The spectral measurements of the Los Alamos pile radiation seem to substantiate this assumption.[3]

measurements, but there are little data[7] on the spectral distribution as a function of time. In view of the discrepancy between different measurements of the time variation of intensity, the fragmentary evidence of King,[7] and the lack of any positive data on the time variation of the spectral distribution, it was considered necessary to include such time resolution in the proposed experiments. Reference 9 gives the detailed reasoning in choosing a time resolution of 1 msec.

1.3.4 Sensitivity Range of Detectors

Because of the preshot uncertainties of many of the variables and because of the desirability of standardizing the detectors for the two stations, the spectrometers must be capable of measuring widely different intensities in the same or different energy channels. The variables include (1) the average number of photons per millisecond per energy channel, (2) the time variation of the number of photons per energy channel, (3) the fraction of fragments visible through the collimator, and (4) the response of the channel. Estimates of item 1 are obtainable only by assuming that the spectrum of the bomb radiation is similar to that from the pile.* Although it is suspected that variables of the types 2 and 3 exist, estimates are only possible by considering limiting cases. Item 4 may be computed from the spectrometer design. Items 1, 2, and 3 are thus almost independent of the type of instrument used, but item 4 can only be determined after the spectrometer design has been completed. The sensitivity range required for each of these variables will now be derived.

The pile measurements, together with the theoretical absorption coefficients, permit an estimate of the photon distribution at the two stations. The pile spectrum[10] indicates that without air attenuation a photon distribution would be expected of the form

$$\frac{N}{N_0} = e^{-1.15E} \qquad (1.1)$$

Where N is the number of photons per kev at an energy E in Mev and N_0 is the number per kev at zero energy. The total absorption coefficient for Eniwetok air may be approximated by

$$\mu = \frac{E^{-1/2}}{140} \qquad (1.2)$$

where E is the photon energy in Mev and μ is the linear absorption coefficient in reciprocal meters. The energy distribution of the photons at a distance L from the bomb in good geometry is thus

$$\frac{N}{N_0} = e^{-[(1.15E + E^{-1/2}L)/140]} \qquad (1.3)$$

The relative number of photons at the two stations may be obtained by summing over a large number of equal energy intervals in the interesting energy range. The pertinent data† for the two stations are listed in Tables 1.1 and 1.2.

For the spectrum experiment measurement of 99 per cent of the photons should be assured. According to Tables 1.1 and 1.2, the neglect of photons which occur above 4.5 Mev for Station 54 and above 6.0 Mev for Station 57 will cause less than a 1 per cent loss.‡ Next the range of detector sensitivity required for these photon energy bands should be determined.

The spectrometer response will depend upon the spectrometer type and design, but for the present purpose the actual design outlined in Chap. 2 will be used to determine the requirements for the detector range. It is estimated that other designs will not reduce this computed relative response requirement by more than a factor of 5. The relative spectrometer response in Tables 1.1 and 1.2 is obtained by multiplying the intensity per energy interval by the Compton electron momentum§ and by the

*See reference 1 for arguments as to the reasonableness of this assumption.

†Inverse-square corrections are not required in these tables because the collimators are approximately the same for the two stations.

‡This neglect is for the purpose of the requirement of sensitivity computations only. Because of the uncertainty of the data from which these computations are made, the spectrometer design will include channels up to 12 Mev. Thus, if there is appreciable intensity in the range above 4.5 or 6 Mev, it will still be measured.

§The photon bandwidth accepted here is proportional to the momentum of the Compton electrons.

conversion efficiency of photons to electrons. The relative number of electrons arriving at the detector is thus listed in column 3 of Tables 1.1 and 1.2. For the energy range proposed in the preceding paragraph the detectors will show relative responses of from 2 to 36 at Station 54 and of from 0.01 to 5 at Station 57. In order to reduce the large response range required by the above figures, it is probably permissible to eliminate the requirement that channels below 1.0 Mev be measured at Station 57. This deletion may increase the counting loss from 1 per cent to perhaps 5 per cent. Under these conditions a range of perhaps 20 is required at each station with an additional factor* of 7 if both stations are to use the same detectors.

There are no adequate data on the time variation of the number of photons per energy channel. The results at Sandstone reported by King[1] indicated that the mean energy varied from perhaps 1.5 to 4.5 Mev in the first millisecond. For this reason alone it was deemed advisable to allow for such a time variation in the detector range requirements for the Greenhouse tests. A factor of 10 was arbitrarily assigned.

TABLE 1.1 ESTIMATES OF RELATIVE SPECTRAL DISTRIBUTION FOR STATION 54

Energy (Mev)	N_1, Photons*	Electrons†
0.5	1470	2
1.0	1250	11
1.5	815	23
2.0	454	27
2.5	346	36
3.0	215	36
3.5	113	28
4.0	63	22
4.5	38	17
5.0	22	13
5.5	11	9
6.0	7	7
6.5	4	4
7.0	2	3
7.5	1	2
8.0	1	1
Total	4812	

*Relative number of photons per unit energy interval.

†Relative number of electrons measured per unit energy interval of photons.

TABLE 1.2 ESTIMATES OF RELATIVE SPECTRAL DISTRIBUTION FOR STATION 57

Energy (Mev)	N_2, Photons*	Electrons†
0.5	10	0.013
1.0	35	0.32
1.5	45	1.5
2.0	50	4.0
2.5	40	4.1
3.0	30	5.0
3.5	19	4.7
4.0	12	4.2
4.5	8	3.6
5.0	5	3.0
5.5	3	2.1
6.0	2	1.7
6.5	1.0	1.1
7.0	0.6	0.8
7.5	0.4	0.6
8.0	0.2	0.3
Total	261.2	

*Relative number of photons per unit energy interval.

†Relative number of electrons measured per unit energy interval of photons.

*This factor results from the air attenuation between Stations 54 and 57.

It is not known how the fission fragments are distributed, but it seems very unlikely that they remain concentrated in a small diameter sphere. Probably the most reasonable guess is that they are distributed uniformly in the ball of fire. It has also been suggested that they may be contained in a thin shell whose radius is that of the ball of fire. The fraction of the fragments visible through the collimator system actually used has been computed in Chap. 2 for each of these cases as a function of time. The maximum variation in this fraction is shown to be a factor of 25 for Station 54 and 35 for Station 57.

In addition to the general trend of spectrometer response with energy there are also variations because the channels used in the final design are not identical. In Chap. 2 a range of response of 3 at a given energy will be obtained for the spectrometer. This factor must be included in the range requirements.

The total sensitivity range for the detectors is thus the product of the above effect or 1.5×10^5. The steps taken to provide this range of sensitivity are outlined in Chap. 2 (physical methods) and in reference 9 (electronic methods).

1.3.5 Scattering

Any type of spectrometer will require a collimated beam and sufficient shielding around the sensing element to reduce extraneous radiation to acceptable levels. Collimators cannot, of course, entirely prevent air-scattered radiation from reaching the spectrometer and thus affecting the measured energy distribution. A correction must be obtained for this scattering. A description of the scale experiments with the results which provide a guide to this correction are given in reference 5. Air-scattered radiation from the active ground may also reach the spectrometer. (Ground activity results from the high neutron flux whose principal component arrives at the ground in much less than 1 msec and from deposited fission materials.)

1.3.6 Intensity Instruments

As each of the spectral measuring instruments is calibrated in absolute terms, it is possible to calculate the intensity rate from their data within the energy range covered. In order to obtain an over-all check of the spectrometer results, it was decided to actually measure the dosage rate in the same geometry as that of the spectrometers. An intensity unit was used for this measurement; the results of this measurement and a full description of the intensity unit are given in reference 14.

1.3.7 Recorders

The type and location of the recorders were decided on the basis of expense, available real estate, and required recording time. A distant recording station would require less sturdy construction to survive the blast and therefore would be less expensive. The cost of cabling to a distant recording shelter, however, compensates for this shelter saving. A final decision on the recording-station location was thus based on available real estate which placed them at 1200 yd from zero on Engebi and 1600 yd from zero on Runit.

Oscilloscope and magnetic tape recorders were initially considered for these tests. Oscilloscopes, however, require photographic film; this means that radiation shielding is very important. Film shrinkage and high-voltage requirements are also perturbing factors with oscilloscopic recording. The greatest disadvantage, however, is that an oscilloscope is required for each record whereas a number of records may be made on a single tape recorder. For these reasons magnetic tape recorders were chosen. Their characteristics are outlined in some detail in reference 11.

REFERENCES

1. Greenhouse Report, WT-107 Ref. 9, Annex 1.2, Part I, Sec. 1.2.1.
2. B. E. Witt, private communication, Los Alamos Scientific Laboratory Report, LAB-J-555, June 23, 1949 (not available).
3. Greenhouse Report, WT-107 Ref. 9, Annex 1.2, Part I, Chap. VI.
4. W. H. Langham et al., Handbook for Biological Experiments at the 1951 Eniwetok Tests, Los Alamos Scientific Laboratory Report, LAB-J-675, Fig. 3 (not available), Oct. 26, 1949.
5. Greenhouse Report, WT-107 Ref. 9, Annex 1.2, Part I, Appendix A.

6. B. E. Watt, Los Alamos Scientific Laboratory, preliminary data.
7. L. D. P. King, Gamma-ray Intensities at the Sandstone Tests in the Region 0-1000 Microseconds, Sandstone Report, Vol. 29, Annex 8, Part II.
8. K. Way and E. P. Wigner, The Rate of Decay of Fission Products, Phys. Rev., 73: 1318-1330 (1948).
9. Greenhouse Report, WT-107(Ref.), Annex 1.2, Part I, Chap. III.
10. Greenhouse Report, WT-107(Ref.), Annex 1.2, Part I, Fig. 6.8.
11. Greenhouse Report, WT-107(Ref.), Annex 1.2, Part I, Chap. IV.
12. Greenhouse Report, WT-107(Ref.), Annex 1.2, Part I, Appendix A.
13. Greenhouse Report, WT-107(Ref.), Annex 1.2, Part I.
14. Greenhouse Report, WT-77, Annex 1.2, Part II.

Chapter 2

Spectrometer Design

2.1 TYPE OF SPECTROMETER

The spectrometer for the Greenhouse tests utilized the Compton process to examine gamma radiation. With a collimated gamma-ray beam incident on a foil (or radiator), the spectrometer was designed to accept only those secondary electrons ejected in a narrow cone in the direction of the beam.[1] Therefore, for monoenergetic photons incident on the foil, the spectrometer accepts Compton electrons from a narrow energy interval out of the continuous Compton distribution. This selection was determined by baffles which were placed at strategic positions along the electron paths. The accepted electron paths were bent by a magnetic field so that the momenta of the electrons reaching a detector were defined by the position of the detector and the value of the magnetic field. The number of Compton electrons ejected per unit time within the spectrometer acceptance angle was measured by the spectrometer detector as a function of the magnetic field. From such measurements the energy spectrum of an incident gamma-ray beam was deduced with the aid of the well-established Klein-Nishina formula.

In addition to measuring the electron intensities, described above, this spectrometer detected positrons created in the radiator by the incident photons. The positrons were measured simultaneously with and in the same energy intervals as the electrons. The data obtained from the positron measurements were used to determine necessary corrections (see Sec. 2.5).

2.2 EXTENT OF ENERGY-RANGE MEASUREMENTS

For the requirements of Operation Greenhouse, it was necessary to measure the complete gamma-ray spectrum as a function of time. To scan the whole spectrum at any given time required that each spectrometer detector see a specified energy interval of the spectrum. In view of the uncertainties of the spectrum, it was desirable to have complete coverage over a large energy range so that the measured energy intervals should be overlapping rather than separated. For reasons discussed in Chap. 1, it was agreed that the total energy range covered should extend from 0.5 to 12 Mev. The thoroughness with which this energy range was covered was limited practically by the number of detectors used.

The acceptance angle of the spectrometer could be fixed by placing a defining baffle near the foil. With this arrangement a continuous photon spectrum would produce a corresponding spread of electrons along a focal curve for a constant magnetic field. Therefore it would be possible to scan a continuous photon energy range by placing detectors at adjacent intervals along this focal curve. Further, the prescribed energy range from 0.5 to 12 Mev could conceivably be covered with one or two spectrometers, depending on the size of the pole face and the detector.

However, measurements made of the Co^{60} gamma radiation with a spectrometer built according to the above design revealed that the presence of the baffle near the radiator produced serious electron scattering. Electrons were also produced in the baffles by the foil scattered photons. The electrons from such effects overshadowed those coming directly from the foil. This condition made it necessary to move the defining baffle away from the proximity of the radiator so that, in effect, the collimation of the secondary electrons would have to be imposed after the electrons were dispersed by the magnetic field according to their

momenta. Consequently, the electron-energy range was divided into separate energy channels by a set of baffles. Each channel accepted electrons confined to a finite momentum interval, and the spacing between channels was determined by the size of the baffles required for each channel.

Because of such factors as cost and real estate, it was desirable to cover the specified energy range with as few spectrometers as possible. The number of spectrometers required depended on the number of channels per spectrometer and the percentage energy spread of each channel. It was agreed at Los Alamos that resolution could be sacrificed in this experiment and that an energy spread of the order of 20 per cent would be permitted for each channel. With this specification about the resolution, it was only necessary to find the maximum number of channels that could practically be included in each spectrometer.

2.3 MAGNETIC FOCUSING METHOD

Preliminary investigations were made of the suitability of the conventional magnetic focusing methods to this problem. For example, one possibility was the uniform field 180° type spectrometer.[2] In this type of spectrometer the source (the radiator in this case) and the detector are both inserted in the uniform magnetic field between the pole faces. To impose this condition on the detector was a definite disadvantage in view of the fact that for these measurements the detector was to be a scintillation counter (Sec. 2.7) which was very sensitive to external magnetic fields. However, a more serious objection to the 180° spectrometer was that it required a large pole-face area for a given energy range; therefore a prohibitive amount of material would be required for the electromagnets in order to cover the specified energy range. (This fact was especially apparent when it was decided that the pole-face area should be doubled to permit the simultaneous measurement of the positron spectrum.) Further, it was found that, for large radii of the electron trajectories, an impractically large area was required for the detector in order that it intercept the specified 20 per cent energy interval. For these reasons it was decided not to use the 180° type spectrometer.

The method of focusing the charged particles with a wedge-shaped magnetic field[3] overcomes the objections of the 180° type spectrometer. This type of focusing is shown in Fig. 2.1. This drawing shows the trajectories for electrons having two different momenta (shown by the radii r_1 and r_2 at a given magnetic field) which define the limits of the percentage momentum spread in a channel. The electrons leave the source (in this case the radiator foil F) and are focused at two different focal points P_1 and P_2. It is seen that the parameters to be determined in this type of focusing are the distances d and L, and the angles ϑ and Φ.

The optimum condition for obtaining as many channels as possible in one spectrometer is that the beam width defined by the extreme rays of r_1 and r_2 in Fig. 2.1 be as narrow as possible. To determine what values of the above parameters would give the narrowest beam width, electron trajectories were drawn for various values of d, L, and Φ. (The value of ϑ was selected to be 5° as a compromise between larger ϑ values which would give higher counting rates and smaller ϑ values which would give a smaller energy spread of electrons due to angle.) It was found that the values which gave the smallest beam width for a given resolution were as follows: d = 0, L = 4 cm, and $\Phi = 105°$. (In order to provide a more nearly uniform field around the foil, it was actually placed 1 in. inside the pole-face region, d = −2.54 cm.) However, even with the above optimum values it was necessary to further reduce this beam width in order that it be less than the maximum detector width. (The detector width is discussed in Sec. 2.7.) Since the beam width was a function of the r values of a particular channel, this reduction was obtained by shaping the pole-face edge AB so that in effect the angle Φ was different for each channel. The resulting shaped pole face is shown schematically in Fig. 2.2. (This figure also shows the baffle system discussed in Sec. 2.4.1.)

The trajectory drawings made for this shaped pole face were checked experimentally by the hot-wire method. In this method a wire is placed in the magnetic field with one end passing through the foil position and the other end through the region of the detector. When current is passed through the wire, the latter assumes the trajectory of an electron trajectory. With

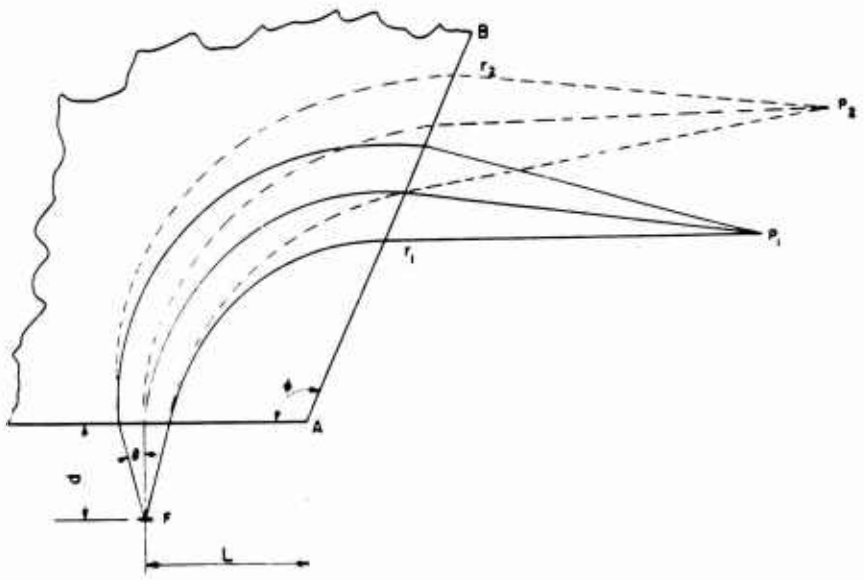

Fig. 2.1 Magnetic Focusing with Wedge-shaped Field

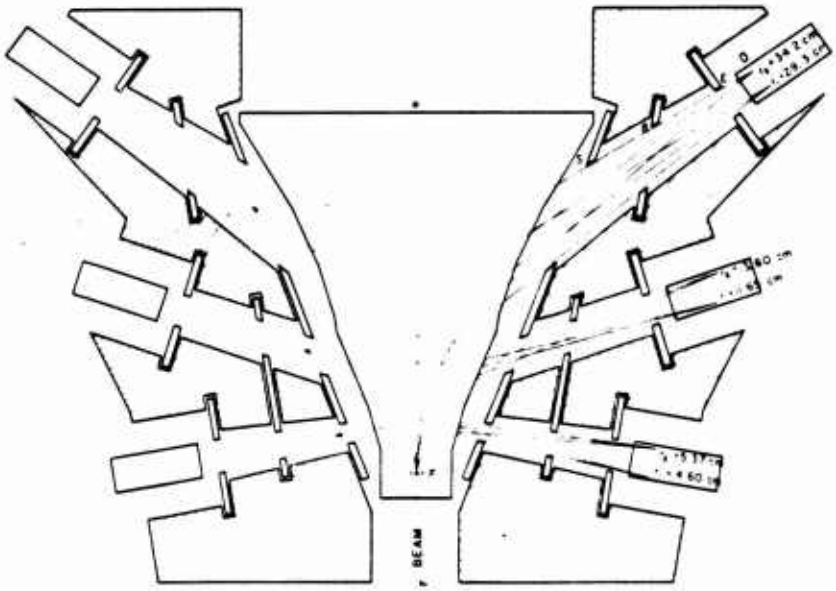

Fig. 2.2 Schematic Drawing of Spectrometer Energy Channels and Pole Face. B and E, baffles, P pole face, D, detector, F, foil.

a suitable adjustment of the magnetic field, the current in the wire, and the tension in the wire, the shape assumed by the wire can be directly compared to the electron trajectories drawn for various r values and angles of ejection. For all the cases that were observed, the trajectory drawings followed very closely the curves assumed by the wire. These drawings, therefore, may be considered as a good first approximation.

2.4 CHANNEL DESIGN

It was found from the trajectory drawings that the most feasible spectrometer design was one which allowed for three energy channels per spectrometer with an approximate momentum spread $\Delta r/r$ of 17 per cent per channel. With this number of channels it required 7 spectrometers (or 19 channels plus 2 repeat channels) to cover an energy range from 0.5 to 12 Mev (gamma-ray energies).

The separation of the channels was designed so that the ratio of the r values for adjacent channels was a constant. For example, in Fig. 2.1, the extreme r values of a single channel are shown by r_1 and r_2. The ratio of the r_1 values (or r_2 values) in two adjacent channels was constant. This constant was chosen in such a manner that the gap in Hr values between the two adjacent channels in one spectrometer was completely scanned by channels of other spectrometers. With such a design the same baffle arrangement could be used for all spectrometers, and it would be necessary merely to use different magnetic-field values with each spectrometer in order that different portions of the energy spectrum be covered. It was found that such a condition was obtained if the constant ratio of r values between channels was chosen to be 2.53 and the percentage momentum spread, defined as $[(r_2 - r_1)/r_1] \times 100$, of each channel was 16.7. The extreme r values of each channel are given in Table 2.1. Also this table gives the magnetic-field values for each spectrometer and the electron-energy intervals covered by each spectrometer. It will be noted in these specifications that the seven spectrometers cover an electron-energy range from 0.323 to 11.87 Mev and that two channels of spectrometer 7 repeat energy intervals covered by other channels.

2.4.1 Baffle Design

The channels of each spectrometer were defined by baffles. A schematic drawing of the spectrometer channels (including three positron channels discussed in Sec. 2.5) is shown in Fig. 2.2. The criteria for the placement of the baffles were that they be sufficiently removed from the direct photon beam and that a minimum surface area be exposed to photons scattered from the radiator. For this reason, the defining slit S (shown in Fig. 2.2) was placed along the pole-face edge.

Considerable scattering effects are introduced at the edges of the baffles. This factor made it desirable to position the defining baffle in the magnetic field so that electrons scattered from the baffle edges would be deflected away from the detector by the magnetic field. This latter feature was not realized in the above design because, as shown in Fig. 2.2, the insertion of the baffle inside the region of the pole faces placed the former too close to the direct photon beam. Another way to reduce the "edge scattering" would be to make the baffle edges as narrow as possible. However, the baffle thickness was determined by the range of 15-Mev electrons. Such a requirement indicated that it was most practical to construct the baffles out of a $\frac{3}{8}$-in.-thick brass plate, in spite of the possible scattering that would be introduced by such edges.

The defining slit S served to determine the extreme r values and the angle of acceptance that could be permitted for each channel. The baffles B and E served to reduce electron scattering. The baffles B and E (Fig. 2.2) were positioned by slots in the spectrometer vacuum chamber; whereas the defining baffle was attached to the edges of the pole faces, P, and accurately positioned with respect to them. The positions of the baffles B and E with respect to the defining baffle were accurately set with the aid of a template.

Because of the wide range of counting rates expected for the various detectors, it seemed desirable to reduce the transmission of certain channels. This reduction in transmission was obtained by inserting a narrow slit baffle directly in front of the detector. The slit width of the baffle was $\frac{1}{8}$ in. in the Z direction (perpendicular to the plane of Fig. 2.2). Choice of such a narrow slit was based on the pile type spec-

TABLE 2.1 ENERGY-CHANNEL ARRANGEMENT FOR SPECTROMETERS

Spectrometer No.	Channel 1 (Bottom) r_1 = 4.60 Cm; r_2 = 5.37 Cm		Channel 2 (Middle) r_1 = 11.65 Cm; r_2 = 13.60 Cm		Channel 3 (Top) r_1 = 29.3 Cm; r_2 = 34.2 Cm		H (gauss)
	Hr (gauss-cm)	Electron Energy (Mev)	Hr (gauss-cm)	Electron Energy (Mev)	Hr (gauss-cm)	Electron Energy (Mev)	
1	2,200	0.323	5,572	1.236	14,020	3.725	478
	2,568	0.413	6,503	1.504	16,350	4.418	
2	2,568	0.413	6,503	1.504	16,350	4.418	558
	3,000	0.524	7,600	1.822	19,100	5.240	
3	3,000	0.524	7,600	1.822	19,100	5.240	652
	3,500	0.656	8,866	2.195	22,300	6.200	
4	3,500	0.656	8,866	2.195	22,300	6.200	761
	4,087	0.816	10,350	2.634	26,070	7.329	
5	4,087	0.816	10,350	2.634	26,070	7.329	888
	4,772	1.008	12,092	3.150	30,380	8.600	
6	4,772	1.008	12,092	3.150	30,380	8.600	1,036
	5,572	1.236	14,117	3.727	35,400	10.110	
7	5,572	1.236	14,117	3.727	35,400	10.110	1,208
	6,480	1.498	16,380	4.426	41,270	11.873	

$$\frac{r(\text{channel 1})}{r(\text{channel 2})} = \frac{r(\text{channel 2})}{r(\text{channel 3})} = 2.53$$

$$100 \times \frac{r_2 - r_1}{r_1} = 16.7 \text{ per cent}$$

trum,[4] which indicated the channels having the highest counting rates. From the data obtained for the pile spectrum, it was decided that the narrow slits would be used in those channels covering an electron-energy range from 0.41 to 2.6 Mev (see Table 2.1) for the spectrometers in Station 54.

2.5 PHOTOELECTRIC AND PAIR-PRODUCTION CONTRIBUTION

This spectrometer was designed to measure the momentum and intensity of secondary electrons ejected in the forward direction from a radiator by an incident photon beam. From such measurements the photon-energy spectrum was deduced on the basis of the Compton process. However, in the specified photon-energy range (0.5 to 12 Mev), the secondary electrons detected by the spectrometer could also include photoelectrons and electrons arising from pair production. Therefore it was necessary to determine the magnitude of these latter contributions and to investigate how such contributions affected the spectrometer design.

The number of photoelectrons detected in an energy channel of the spectrometer with a beryllium radiator was expected to be negligible compared to the number of Compton electrons detected. For example, this comparison can be made for the worst case at the lowest photon energy of 0.5 Mev where the photoelectric cross section is the largest. Heitler[5] indicates that the total photoelectric cross section for carbon ($Z = 6$) is approximately 2×10^{-28} cm^2 per atom at 0.5 Mev. On the other hand the Compton cross section for electron emission into the 5° acceptance angle of the spectrometer is approximately 3×10^{-26} cm^2 per atom. These values indicate that the number of photoelectrons accepted by the spectrometer were certainly less than 1 per cent of the Compton electrons, especially for a radiator with a lower atomic number than 6 such as beryllium ($Z = 4$).

In the case of the pair-production process, the problem of determining the number of negatrons accepted by a spectrometer energy channel is rather involved. An electron may be produced by the pair-production process with a kinetic energy of anything from zero up to that of the photon energy -1.02 Mev. As a result a single energy photon may put a pair-produced electron in any of the channels of the spectrometer. In order to compute a correction to the electron intensities obtained in a given channel, it is necessary to know the spectral distribution of photons and the differential cross section of the pair-production process. Although the spectrum from a bomb is not known, reasonable assumptions may be made (based on the results of pile measurement) to obtain an estimate of the contribution expected from the pair-production process.

It will be assumed as a first approximation that the spectrum to be measured is continuous over a specified energy range and has the form*

$$N(k) = N_0 \left(-k \frac{2}{29} + \frac{30}{29} \right) \qquad (2.1)$$

between 0.5 and 15 Mev, where N is the number of photons per Mev incident on the radiator per cm^2 per sec and k is the photon energy in Mev units. With such a photon beam incident on the radiator, the number of negatrons $n_{p.p.}$ created per nucleus with an energy between E^- and $E^- + dE^-$ can be written as

$$n_{p.p.}(E^-)\, dE^- = dE^- \int_{E^- - m_e c^2}^{15} \phi(E^-,k)\, N(k)\, dk \qquad (2.2)$$

where $\phi(E^-,k)$ is the cross section for such a process, E^- includes the rest energy of the negatron, and N is defined in Eq. 2.1. The values of this cross section as a function of the incident photon energy k and the negatron energy E^- are obtained from the Bethe-Heitler calculations.[6]

The number of these pair-produced negatrons which fall within the accepted energy range of a channel with mean energy E is then

$$\int_{E-(\Delta E/2)}^{E+(\Delta E/2)} n_{p.p.}(E^-)\, dE^-$$

where ΔE is simply related to the resolution of the channel. This result is presented in Table

* The spectrum was assumed to have the form given in Eq. 2.1 rather than Eq. 1.1. Equation 2.1 was used as a sample to describe the spectrum before any pertinent experimental data had been obtained.[4] It assumes that the spectrum has a high energy cutoff at 15 Mev rather than the exponential falloff given in Eq. 1.1. Therefore, for Eq. 2.1, the contribution expected from pair production will be a high estimate.

2.2. It does not follow that a particular channel will receive all the pair-production negatrons having energies in the range defined by this channel. In fact, only a fraction of this number is received by the channel. This condition arises because of the relatively wide angular distribution of the negatrons (which is a function of the incident photon energy) as compared to the small acceptance angle (approximately 5°) of the spectrometer. The fraction of negatrons that is included in a 5° angle can be roughly estimated for the various energy channels from some recent experimental results.[7] This fraction is expressed in Table 2.2 as a percentage P for the nine selected energy channels. Finally, from the percentage P and the number of negatrons in the desired energy range, the number of negatrons $\tilde{n}_{p.p.}$ accepted by a particular channel is calculated as in Eq. 2.2 and is given in the last column of Table 2.2.

The number of negatrons $\tilde{n}_{p.p.}$ is to be compared with the number of Compton electrons n_c accepted in the particular channel for the simplified type of photon spectrum given by Eq. 2.1. The number of Compton electrons n_c accepted in a particular channel for Z scattering centers may be expressed approximately as

$$n_c = Z \int_{k_1}^{k_2} N(k)\, dk \left[2\pi \int_0^{\theta(k)} \sigma(k,\theta) \sin\theta\, d\theta \right] \quad (2.3)$$

where $\sigma(k,\theta)$ is the Klein-Nishina differential cross section, k is the energy in Mev units of the incident photon, k_1 and k_2 are the photon energies that correspond to the extreme Compton electron energies (shown in Table 2.1) accepted in a 5° cone for a particular channel, and θ is the angle of photon scattering corresponding to electron ejection at an angle of 5° with the forward.[8] (This calculation of the expected response of the various channels is discussed in considerable detail in reference 8.) The variation of the energy of the Compton electrons with the angle of ejection will be neglected as a first approximation because of the small acceptance angle.

TABLE 2.2 PAIR-PRODUCTION NEGATRONS ACCEPTED BY SPECTROMETER CHANNELS

Spectrometer No.	Channel No.	E (Mev)	ΔE (Mev)	$\int n_{p.p.}\, dE^{-}$*	P†	$\tilde{n}_{p.p.}$*†§
2	1	0.928	0.111	0.252 N_0	3	0.00856 $N_0\bar{\phi}$
4	1	1.166	0.150	0.395 N_0	3	0.0134 $N_0\bar{\phi}$
6	1	1.518	0.228	0.532 N_0	8	0.0437 $N_0\bar{\phi}$
2	2	2.014	0.318	0.795 N_0	18	0.141 $N_0\bar{\phi}$
4	2	2.705	0.439	0.974 N_0	18	0.173 $N_0\bar{\phi}$
6	2	3.660	0.577	1.036 N_0	33	0.346 $N_0\bar{\phi}$
2	3	4.928	0.822	1.170 N_0	33	0.390 $N_0\bar{\phi}$
4	3	6.710	1.129	0.904 N_0	43	0.387 $N_0\bar{\phi}$
6	3	9.110	1.510	0.535 N_0	57	0.305 $N_0\bar{\phi}$

* N_0 is a constant multiplier in the assumed photon spectrum incident on the radiator foil and has dimensions of $cm^{-2}\ sec^{-1}$.

† P = percentage of negatrons accepted by spectrometer.

‡ $\tilde{n}_{p.p.} = P/100 \int n_{p.p.}\, dE^{-}$.

§ $\bar{\phi} = Z^2 r_0^2/137 = 5.71 Z^2 \times 10^{-28}\ cm^2$.

The results of the calculations of n_c based on Eq. 2.3 for the particular channels chosen in Table 2.1 are given in Table 2.3. In this table the value of the cross section $\sigma(k)$, defined as

$$\int_0^{\theta(k)} \sigma(k,\theta)\, 2\pi \sin\theta\, d\theta$$

is taken to be the average value over the energy interval from k_1 to k_2.

TABLE 2.3 COMPTON ELECTRONS ACCEPTED BY SPECTROMETER CHANNELS

Spectrometer No.	Channel No.	Electron-energy Range (Kinetic Energy, Mev)	Incident Photon-energy Limits k_1	k_2	$\int_{k_1}^{k_2} N\,dk^*$	$\sigma(k)$ (cm^2/electron)	n_c
2	1	0.413–0.524	0.58	0.67	0.111 N_0	0.55 $\times 10^{-26}$	0.061 N_0Z $\times 10^{-26}$
4	1	0.66–0.82	0.87	1.01	0.157 N_0	0.60 $\times 10^{-26}$	0.094 N_0Z $\times 10^{-26}$
6	1	1.01–1.24	1.23	1.45	0.218 N_0	0.68 $\times 10^{-26}$	0.148 N_0Z $\times 10^{-26}$
2	2	1.50–1.82	1.72	2.05	0.292 N_0	0.85 $\times 10^{-26}$	0.248 N_0Z $\times 10^{-26}$
4	2	2.20–2.63	2.47	2.86	0.382 N_0	1.03 $\times 10^{-26}$	0.394 N_0Z $\times 10^{-26}$
6	2	3.15–3.73	3.38	3.96	0.46 N_0	1.25 $\times 10^{-26}$	0.57 N_0Z $\times 10^{-26}$
2	3	4.42–5.2	4.65	5.48	0.58 N_0	1.45 $\times 10^{-26}$	0.84 N_0Z $\times 10^{-26}$
4	3	6.20–7.23	6.45	7.58	0.64 N_0	1.62 $\times 10^{-26}$	1.03 N_0Z $\times 10^{-26}$
6	3	8.60–10.1	8.9	10.4	0.66 N_0	1.70 $\times 10^{-26}$	1.12 N_0Z $\times 10^{-26}$

* N_0 is a constant multiplier in the assumed photon spectrum incident on the radiator foil and has dimensions of cm^{-2} sec^{-1}.

The percentage of pair-production negatrons compared to the total number of secondary electrons detected in a particular spectrometer channel is stated in Table 2.4. The channels given in this table are the same as those in Tables 2.2 and 2.3. The values of $\tilde{n}_{p.p.}$ and n_c are given in Tables 2.2 and 2.3 for an incident photon beam and for a single atom (atomic charge of Z). As a basis of comparison, percentage calculations were made for aluminum (Z = 13) and for beryllium (Z = 4). It is seen in Table 2.4 that these percentages are not negligible. For example, in channel 6-2, the percentage of pair-production negatrons would be 12 for a beryllium radiator and 31 for an aluminum radiator. These calculated results led to two conclusions regarding the design of the spectrometer: (a) it was desirable to provide some experimental means of correcting for the pair-production negatrons detected in a given channel, and (b) it was desirable to use a low Z radiator such as beryllium rather than a material like aluminum.

TABLE 2.4 COMPOSITION OF ELECTRONS ACCEPTED BY SPECTROMETER CHANNELS

Spectrometer No.	Channel No.	Electron-energy Range (Kinetic Energy, Mev)	Percentage of Pair-production Negatrons*	
			Z = 13 (Al)	Z = 4 (Be)
2	1	0.413–0.524	9	3
4	1	0.65–0.81	9	3
6	1	1.00–1.23	18	6
2	2	1.50–1.82	30	12
4	2	2.20–2.63	25	9
6	2	3.15–3.73	31	12
2	3	4.41–5.24	25	9
4	3	6.20–7.23	21	7
6	3	8.60–10.11	16	6

*$[\tilde{n}_{p.p.}/(n_c + \tilde{n}_{p.p.})] \times 100$; see Tables 2.2 and 2.3.

As a method of correction for pair-production negatrons, it was decided to provide each spectrometer with three additional energy channels. These latter channels were designed exactly like the original three channels but were symmetrically positioned on the opposite side of the pole faces. With this arrangement and with the direction of the magnetic field fixed, one set of channels measured negatrons, and the other set measured positrons; further, two opposite channels detected particles in the same energy interval. If it is assumed from the Bethe-Heitler theory[5] that there is approximately the same probability of finding a positron as a negatron in a given energy interval and that the angular distribution is the same for positrons as for negatrons, then the number of positrons detected in a positron channel will be a measure of the number of pair-production negatrons detected in the corresponding opposite channel. Another feature of these positron channels is that they provide a means of correcting for the background intensity, which is expected to be considerable. Therefore, if the measured intensity of the positron channel is subtracted from that of the corresponding negatron channel, the errors due to background and pair-production negatrons are both corrected. The experimental layout of these six channels in the spectrometer is shown schematically in Fig. 2.2.

2.6 SPECTROMETER RADIATOR

The previous calculations have shown that it was desirable to use a low Z material as a

radiator in order to minimize the error due to pair production. A further advantage was that such a material also minimizes the energy loss and scattering of the Compton electrons in the foil. For these reasons beryllium was chosen as the radiator material.

The beryllium foil was placed inside the pole-face gap, 1 in. from the end of the pole face along its center line (see Fig. 2.2). The foil was mounted on an aluminum frame (Fig. 2.3) that was attached to two brass spacers for the pole faces. The length of the foil was 1 in. in order to fit inside the 1-in. pole-face gap. This foil was placed in line with the collimator axis so that it was exposed to the collimated gamma-ray beam. For this gamma-ray beam it was desirable to have a maximum number of Compton electrons ejected from the radiator in order to get good statistics in the allotted time and to get high intensities that were well above background. This condition was obtained by presenting the maximum number of scattering centers to the incident gamma-ray beam or, in effect, by using a foil with a maximum width and thickness. However, the factor which limited the increase of the foil width and thickness is the effect that is produced on the spectrometer resolution.

The optimum foil width and thickness were determined from measurements made of the spectrometer resolution with foils of different dimension. The foil size selected was the maximum size that did not seriously affect the resolutions. The resolution was determined from the half-width of the line shape obtained when monoenergetic photons (0.661-Mev gamma ray from Cs^{137}) were incident on the foil. Line shape measurements were made with foil widths of 4, 8, and 12 mm and with foil thicknesses of 6, 12, and 18 mils. From these measurements the optimum foil dimensions were found to be 12 mils thick and 8 mm wide.

2.7 SPECTROMETER DETECTOR

The detector used in the spectrometer had to satisfy certain requirements. The primary requirement was that it be able to measure a relatively wide range of electron intensities (see Sec. 1.3.4). For this reason the Geiger counter could not be used since it has a relatively long resolving time and it saturates readily at counting rates of the order of 20,000 cpm. On the other hand the scintillation counter is much more desirable in this respect. This type of counter has a relatively short resolving time (of the order of 10^{-8} sec), and, for counting rates that exceed the resolving time, the counter can be used with associated electronic equipment as an integrator which measures total charge collected on the photomultiplier anode in a given time interval. Therefore the scintillation counter was chosen for these measurements in preference to other types of detectors.

2.7.1 Photomultiplier

The photomultiplier tube selected as part of the scintillation detector was the RCA 5819. This tube was used in preference to other photomultipliers because of its large photosensitive surface, which would be desirable for the purpose of intercepting the wide electron beam of a given spectrometer energy channel. Another feature of this tube (to be found in the later model) is that the high-voltage connector is brought out of the base of the tube so that the glass envelope can be used conveniently inside a vacuum chamber.

2.7.2 Effect of Magnetic Field on Photomultiplier

One difficulty that is faced in using the scintillation counter is the inherent sensitivity of the photomultiplier tube to external magnetic fields. This characteristic can become quite serious for calibration measurements that require a wide range of values for the magnetic field. Fortunately there are various steps that can be taken to minimize this change in tube sensitivity with magnetic field. One method would be to completely remove the photomultiplier from the region of the magnetic field. This could be done, as proposed in the preliminary spectrometer design, by fastening a suitable crystal to one end of a Lucite rod and then "piping" the light pulses produced in the crystal through the rod to the photomultiplier tube which is situated outside the region of the magnetic field. However, the Lucite rod imposes an added complication which was avoided by more direct methods. The removal of the photomultiplier from the magnetic-field region was par-

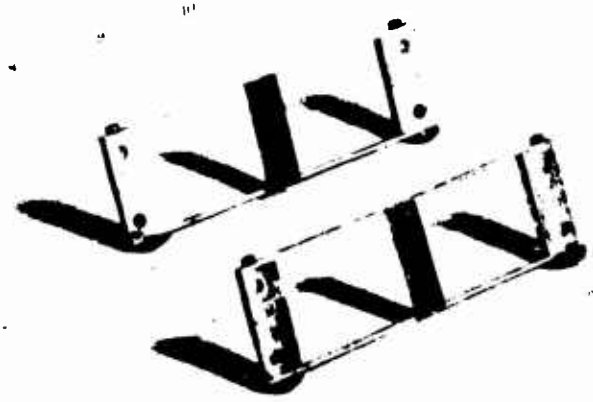

Fig. 2.3 Beryllium Radiators for the Spectrometer

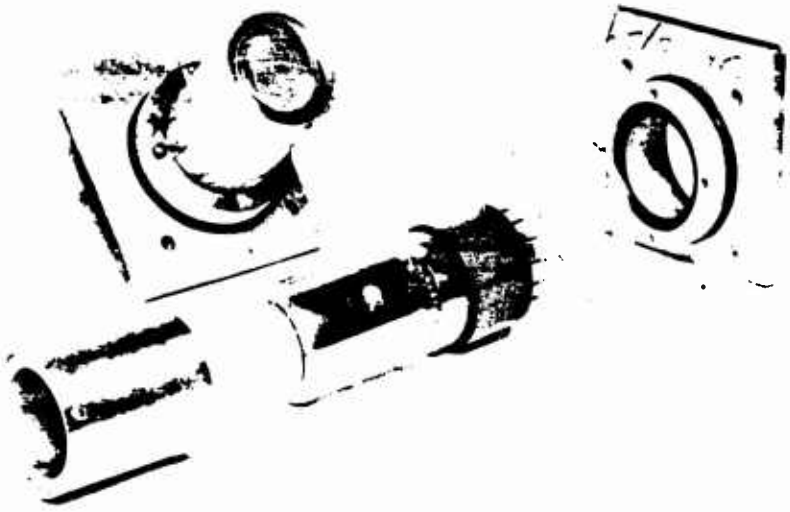

Fig. 2.4 Scintillator Detector and Components

tially accomplished by the use of the wedge-shaped magnetic focusing method discussed previously. With this focusing arrangement (see Fig. 2.2) there was a maximum field of 10 gauss in the region of the photomultiplier tube when a field of 1400 gauss was obtained in the pole-face gap. The situation was further improved by the use of a magnetic shield. It was found that, when a $\frac{3}{16}$-in.-thick Mumetal shield was mounted around the tube electrodes, the maximum field in the region of the electrodes was less than 2 gauss. Figure 2.4 shows a view of the Mumetal shield mounted around the photomultiplier tube.

In addition to these precautions taken to minimize the magnetic field in the vicinity of the detector, it was also possible to considerably reduce the effect of a given magnetic field on the tube behavior. For example, because of the fact that the tube sensitivity to an external magnetic field was very much dependent on the orientation of the plane of the tube electrodes with respect to the direction of the field, it was possible to find an optimum tube position in which this sensitivity was a minimum. Such a position was found by rotating the tube in the presence of a radioactive source and by measuring the counting rate as a function of magnetic field for various tube positions. From such measurements the tube position that gave the smallest variation in counting rate for different magnetic fields was selected as the optimum tube position.

Besides tube orientation, another method of reducing the tube sensitivity to magnetic fields was to increase the first-stage voltage so that the electric field exerted more influence on electrons ejected from the photocathode. The maximum first-stage voltage that could be used was dependent upon the stability of the tube and the permissible background. Measurements were taken to determine the sensitivity of the detector to external magnetic fields for first-stage voltages of 90, 157.5, and 292.5 volts. It was found that there was a much smaller effect of external magnetic fields for the larger first-stage voltages. From the data obtained, it was found desirable to use a first-stage voltage of 200 volts ± 10 per cent in order to minimize the variation in tube sensitivity with magnetic field and at the same time to maintain stable tube operation. Finally, measurements were taken of the counting rate as a function of magnetic field for the case where the three steps discussed above (magnetic shield, tube orientation, and first-stage voltage) were combined. The resulting variation in the counting rate with magnetic field over a range from 0 to 1400 gauss was less than 2 per cent.

2.7.3 Selection of Crystal

The selection of a crystal to be used with the photomultiplier tube involved certain considerations. The available phosphorescent crystals are broadly classified in two groups: organic and inorganic. The inorganic crystals usually possess certain properties which make them undesirable in this particular case. For example, most of these crystals have a relatively high vapor pressure and are hygroscopic; further, they have less transparency and a lower light yield per incident particle. In addition, these crystals usually have a relatively long light decay constant. The above factors were also the basis for eliminating many of the organic crystals. In the last analysis the organic crystal that proved to be the most desirable with respect to the above properties was anthracene. Therefore anthracene was selected as the scintillator material in spite of the fact that anthracene crystals were relatively hard to grow and could be cut only with great difficulty.

The size and shape of the crystal were determined on the basis of the following considerations. It was necessary that the anthracene crystal have the form of a disk with a $1\frac{1}{2}$-in. diameter to cover the photosensitive surface of the RCA 5819 photomultiplier tube, as well as to intercept the electron beam width of a given channel. The thickness of this crystal was determined on the basis of the maximum energy loss that an incident electron would suffer in passing through such a thickness. This energy loss determines the pulse height that is produced by the photomultiplier. If the crystal thickness has such a value that the energy loss of the electron is less than its total kinetic energy, then it is expected that the variation in pulse height with energy will be small. For this reason it was decided to select a crystal thickness which produced an energy loss that was less than most of the electron energies to be measured. However, it was important that

the pulse height resulting from this energy loss be large compared to the average background pulse heights in order to be able to discriminate against the latter. It was found that an energy loss of the order of 1 Mev would produce pulse heights sufficiently greater than the background pulse heights. Such an energy loss corresponds to a crystal thickness of approximately $\frac{1}{8}$ in. Therefore the final dimensions of the anthracene crystal were a diameter of $1\frac{1}{2}$ in. and a thickness of $\frac{1}{8}$ in. Crystals made according to these specifications were provided by The Harshaw Chemical Co. Great difficulty was experienced in growing and cutting these crystals. For example, many of the crystals had cracks and were pitted. The criterion for accepting a crystal was its performance as shown by a bias curve which indicated the distribution of pulse heights for monochromatic electrons incident on the crystal.

The crystal was fixed in front of the photosensitive surface of the tube with the aid of a Lucite adaptor. The adaptor was simply a Lucite disk with a concave surface (4-in. radius) to fit the curved surface of the glass. (The thickness of the Lucite disk at the center was $\frac{1}{32}$ in.) The Lucite was cemented to the glass, and the crystal was cemented to the Lucite with unsaturated polyester resin.

2.7.4 Crystal Reflector

It was desirable that the pulse height obtained for a given energy electron incident on the crystal be as large as possible to increase discrimination against noise pulses. For this reason the effect of an aluminum reflector on the outside surface of the crystal was investigated. An aluminum foil 0.4 mil thick was used to cover the outside surface of the crystal. The counting rate as a function of discriminator volts was measured with and without the foil when monoenergetic electrons were incident on the crystal. The results of this measurement are seen in Fig. 2.5. It is seen that the pulse height (point of falloff from the plateau) without the foil is approximately 60 per cent of that obtained with the foil. For this reason it was decided that each crystal would be covered with a light reflector made of 0.4-mil-thick aluminum foil. This foil was fixed to the face of the crystal with a thin film of silicone grease. A view of the complete scintillator detector is shown in Fig. 2.4.

2.8 SPECTROMETER ELECTROMAGNET

To measure electron energies up to 12 Mev, it was necessary to produce a maximum magnetic field of 1400 gauss in the pole-face air gap. Accordingly it was necessary to design a magnet to produce such a maximum field. It was desirable to make the over-all dimensions of this magnet as small as possible in order to conserve space.

Because of the problem of stabilization the preliminary spectrometer design specified that the desired magnet fields be produced by permanent magnets. These permanent magnets were designed so that the legs leading to the pole faces were made out of Alnico cores, and the remainder of the magnetic circuit material (yoke) was made out of cold-rolled steel. Small soft-iron bars (keepers) were to be shunted across the Alnico cores to permit fine adjustment to the magnetic field. However, the design using these permanent magnets was abandoned in favor of electromagnets for the following reasons: (1) the industrial firm that had contracted to fabricate the permanent magnets did not cooperate in meeting the time limits, (2) the price was excessive, and (3) the electromagnet had more flexibility with respect to the calibration measurements, even though it introduced the extra problem of stabilization.

The size of the coils and yoke of the electromagnet depended to a large extent on the pole-face area and the pole-face gap separation. This size is considerably reduced as the latter two parameters are decreased. The pole-face area was kept from being excessively large by designing the shape for only three energy channels and by using the wedge-shaped rather than the 180° uniform field type of magnetic focusing. The final area obtained for the pole face was approximately 130 sq in. In the case of the pole-face gap separation, it was found desirable to limit this distance to 1 in. Such a relatively small gap separation made it impractical (especially from the viewpoint of the wall scattering that would be introduced) to insert the spectrometer vacuum chamber inside of the gap. Rather it was decided to have the pole faces serve as an integral part of the vacuum chamber with their inside surfaces defining the height of the chamber. The outside surfaces of the pole faces contained gaskets (see Fig. 2.6) for vacuum seals to the aluminum side plates of

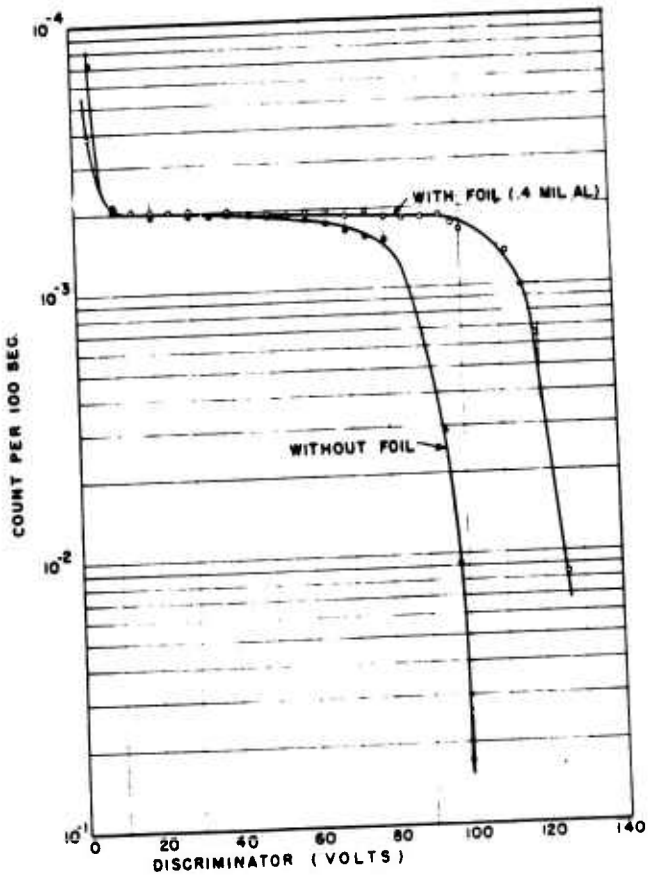

Fig. 2.5 Effect of Aluminum Reflector on Pulse Heights

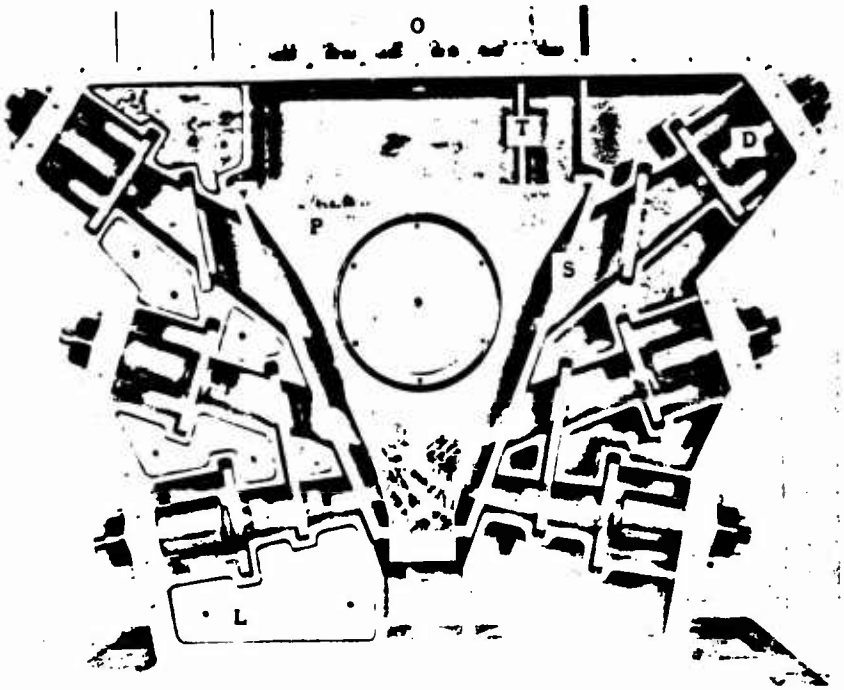

Fig. 2.6 Inside View of Spectrometer Vacuum Chamber. D, detector. L, cover. Q, exit channel for gamma beam. P, pole face. S, defining slit. T, fluxmeter tube.

the chamber. The pole faces made contact with the yoke of the electromagnet through holes in these side plates (see Fig. 2.7). The material of the pole faces was hot-rolled steel which was machined down to a thickness of $1\frac{3}{8}$ in.

The yoke of the electromagnet (Fig. 2.7) was also machined from hot-rolled steel. The thickness of this steel was 2 in., and the width was 8 in. The over-all dimensions of the yoke along the outside legs were 22 in. wide and $21\frac{5}{8}$ in. long. The legs of the yoke which led to the pole faces and served as the core for the electromagnet coils were $4\frac{1}{2}$-in.-diameter rods of hot-rolled steel.

The electromagnet coils were wound on brass spools which slipped over the $4\frac{1}{2}$-in.-diameter rods of hot-rolled steel. These spools were positioned adjacent to each pole face in order to minimize flux leakage and to provide the most efficient design. Each spool was layer wound with approximately 5500 turns of No. 16 double-coated Formex wire. The resistance of each coil was approximately 50 ohms.

Measurements of the magnetic field in the pole-face air gap were made with a rotating coil fluxmeter. The fluxmeter coil consisted of 325 turns of No. 36 wire wound on a rectangular Lucite form ($\frac{5}{32}$ in. $\times$ $\frac{3}{32}$ in.). This coil was attached to the end of a long shaft which was rotated by a Bodine synchronous motor (1800 rpm, $\frac{1}{75}$ hp). A carbon commutator and carbon brushes converted the output voltage of the coil, which was then measured with a microammeter. The fluxmeter was calibrated in a standard magnetic field known to an accuracy of better than 0.01 per cent. The over-all accuracy of the fluxmeter measurement for a given magnetic field was better than 2 per cent. The fluxmeter coil was inserted in the pole-face air gap through a brass reentrant tube leading into the vacuum chamber (see Fig. 2.6).

The current for the electromagnet coils was supplied by 6-volt storage cells. These cells proved to be very stable during a run, especially since it was found necessary to draw currents not exceeding 0.6 amp. The maximum magnetic field produced in the air gap of the pole faces is 1400 gauss with a current of 0.6 amp. This low current requirement made the use of batteries in the field quite feasible and reduced the requirements of auxiliary electronic equipment for stabilization purposes.

2.9 SPECTROMETER VACUUM CHAMBER

It was necessary to design the vacuum chamber of the spectrometer so that in the process of assembly a relatively simple procedure could be followed. To permit ease of assembly, the design features indicated below were adopted. The interior of the chamber contained slots into which the baffles could be inserted. The baffles were held in the slots by setscrews, which were wedged into the walls of the slots. These setscrews permitted accurate adjustment of the baffle position according to a template which prescribed each baffle position with respect to the defining baffle. (This defining baffle was in turn accurately positioned to each exit side of the pole faces; see Fig. 2.6.) Another feature of the chamber was that the empty space between the channels (defined by the baffles) was to be filled with lead. To make the lead protection the same for all spectrometers, it was decided to use lead castings which could be formed to fit in the various available spaces. The various shapes of these lead castings are shown in Fig. 2.6. Further, the chamber was to be designed with six openings for the spectrometer detectors. Through each opening it was intended that a detector could be removed as an integral unit. This detector unit would be provided with an O-ring gasket for a vacuum seal with the walls of the opening. A complete detector unit is shown in Fig. 2.4, broken up into its component parts (including the detector and the plate for holding the detector) and assembled as an integral unit.

At the back end of the vacuum chamber (Fig. 2.6), it was necessary to provide an opening for the exit window, O, through which the gamma-ray beam emerged. This exit window consisted of an aluminum plate which was milled down to a $\frac{1}{64}$-in. thickness over a $1\frac{1}{2}$-in.-diameter area at its center and which contained an O-ring-gasket seal. Adjacent to this exit port an opening was provided for the fluxmeter reentrant tube (Fig. 2.6). The reentrant tube passed through an O ring in an aluminum cover plate which contained an additional O ring to seal the opening in the vacuum chamber. This latter opening in the vacuum chamber for the reentrant tube was made on each side of the exit window because the yoke of the spectrometer magnet would obstruct one of these openings.

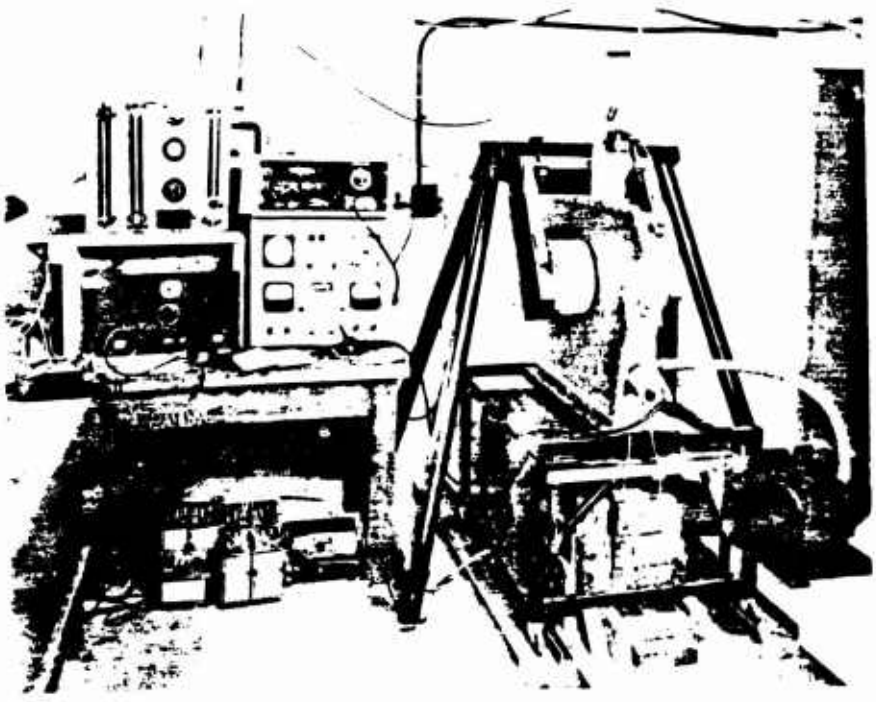

Fig. 2.7 Experimental Arrangement of Spectrometer for Gamma-ray Measurements of Radioactive Source

At the front end of the vacuum chamber, an opening was provided for the entrance window of the gamma-ray beam. Like the exit window this entrance window also consisted of an aluminum plate with the $1\frac{1}{2}$-in.-diameter area at its center, milled down to a thickness of $\frac{1}{64}$ in. However, when the incident gamma-ray beam impinged on this window, a considerable number of secondary electrons could be ejected in such a direction that they would be detected by the spectrometer and therefore cause considerable error in the measurements. For this reason it was necessary to interpose an auxiliary magnetic field just inside the window so that the electrons ejected from the window would be swept aside. This auxiliary field was produced by a small permanent magnet having a $\frac{3}{4}$-in.-gap separation with a magnetic field of approximately 1500 gauss in the gap. This magnet was placed in a container which had the entrance window on one end and an O-ring gasket on the open end which was attached to the front face of the vacuum chamber. An inside view of the container, showing the gasket, magnet, and entrance window, is given in Fig. 2.8.

Because of the large number of spectrometers required, it was necessary that the vacuum chambers be designed so that they could be easily fabricated. For this reason it appeared most feasible to make the chambers in the form of castings. Such castings could be readily fabricated with the necessary slots on the inside as an integral part of the casting. Further, these slots could constitute part of a weblike structure that would hold the lead castings. In view of the requirement that the material of the vacuum chamber must be nonmagnetic, it was decided to make the castings out of aluminum. The use of aluminum involved the risk of porosity, blowholes, or cracks, which would result in air leaking through the casting walls. However, it was found that castings which were reasonably free from these latter defects could be made from an aluminum alloy consisting of 5 per cent silicon and 95 per cent aluminum. A pattern was prepared for the castings which allowed for shrinkage and for the machining of surfaces. The surfaces that were to be machined were the mounting surfaces and the surfaces making contact with the neoprene gaskets.

A view of the interior of the completed vacuum chamber casting is shown in Fig. 2.6. This picture clearly shows the webbing which comprised the slots for the baffles and for the lead castings. The webbing was designed so that it did not require any machining. The height of the webbing was $\frac{1}{4}$ in. below the top of the machined surface in order to facilitate evacuation of the chamber. The pumping port for the chamber was situated at the back side of the casting near the front end. The machined surface around the edge of the box made contact with the gasket of the cover plate which was rigidly fastened with $\frac{1}{4}$-20-stainless-steel bolts. For the screw positions which were above the bosses on the sides of the casting (these bosses contained the openings for tubes, etc., into the vacuum chamber), it was necessary to use stainless-steel studs. It will be noted that the front end of the casting is flanged. The front face of this flanged section was machined and matched to a similar plate which formed the end of the collimator. The vacuum chamber was mounted by this flanged end to the collimator plate, and the axis of the chamber (leading from the center of the entrance window to that of the exit window) was lined up with the collimator axis by means of two dowel pins on the ends of the matching plates.

In addition to the vacuum chamber, it was decided that the photomultiplier tube holders and the sweep magnet holders also would be machined out of aluminum castings. Views of the machined castings for the photomultipliers and for the sweep magnet are shown in Figs. 2.4 and 2.8. These castings fitted over the openings of the vacuum chamber and could be fastened by means of $\frac{1}{4}$-20 studs provided around the openings.

The depth of the vacuum chamber was $3\frac{3}{4}$ in. to correspond to the width of the two pole faces. As shown in Fig. 2.6, each pole face contained an O-ring gasket which provided the vacuum seal around the $6\frac{1}{16}$-in.-diameter opening leading out of each side of the chamber to the magnet yoke. The pole faces were accurately positioned in the chamber by the six screws which fastened the back pole face to the chamber. These screws were laid out with a template so that they lined up the central axis of the pole face (along its length) to the axis of the box (entrance window to exit window). With the

Fig. 2.8 Sweep Magnet Assembly

cover plate of the chamber in place, the magnet yoke could be slipped around the side of the box until it made contact with the extended shoulders of the pole faces (Fig. 2.7). (The base of the magnet yoke had slotted screw holes so that the coil legs could be moved closer together until they butted against the pole faces.)

REFERENCES

1. G. D. Latyschev et al., Recoil Electron Spectrum of Gamma Rays from RaC, J. Phys. U.S.S.R., 3: 251 (1940).
2. J. L. Lawson and A. W. Tyler, The Design of Magnetic Beta-ray Spectrometer, Rev. Sci. Instr., 11: 6 (1940).
3. W. E. Stephens, Magnetic Refocusing of Electron Paths, Phys. Rev., 45: 513 (1934).
4. Greenhouse Report WT-107(Ref.), Annex 1.2, Part I, Chap. VI.
5. W. Heitler, "The Quantum Theory of Radiation," 2d ed., p. 124, Oxford University Press, New York, 1949.
6. W. Heitler, "The Quantum Theory of Radiation," 2d ed., p. 199, Oxford University Press, New York, 1949.
7. H. W. Koch and R. E. Carter, Determination of the Energy Distribution of Bremsstrahlung from 19.5 Mev Electrons, Phys. Rev., 77: 165 (1950).
8. Greenhouse Report WT-107(Ref.), Annex 1.2, Part I, Chap. V.
9. Greenhouse Report WT-107(Ref.), Annex 1.2, Part I, Fig. 2.9.

Chapter 3

Results

3.1 INVENTORY OF DATA

A preliminary examination of the records revealed the extent to which information had been transmitted to the magnetic tape from the various channels. Table 3.1 indicates whether or not each channel had received any signal at all and whether any preshot calibration was obtained. (No data were obtained for Station C-54.) In addition, an estimate of the experimental error arising from the calibration requirements[1] is given for the various energy channels from the available data. The position of each channel and the spectrometer position are shown in Fig. 3.1. The method of evaluation of the data in terms of the experimental accuracy and the conversion from pulse separation to counts per second are given in reference 1.

3.1.1 Recovery of Data from Magnetic Tapes

The information on the magnetic tapes was contained in the interval between successive pulses of magnetization as measured by the number of oscillations of a time reference signal recorded on the same tape. The procedure described herein covers the conversion of the tape data to counts per second in each spectrometer energy channel. It will be recalled that the number of electrons or positrons incident on the PMT crystal per unit time was measured by the current flowing in the anode circuit of the photomultiplier detector. This current determined the voltage developed across a compression circuit whose transfer characteristic was approximately logarithmic, and the voltage in turn determined the interval between successive pulses from a pulse frequency modulator. This modulator had the characteristic that the interval decreased in a linear manner with increasing negative voltage input. The linearity of the modulator to 0.2 per cent (1 per cent full scale of decade) had been established experimentally and theoretically; therefore the critical parameters of the modulator were the slope of the interval vs voltage curve and its intercept with the zero voltage line. Data recovery consisted in performing the reverse task of determining the current in the photomultiplier from given time intervals between pulses. In the discussion of this process the following terms will be used:

Slope: Slope of the curve of interval vs input voltage.

Signal Interval: Interval between pulses in microseconds, corresponding to a counting rate at the detector.

Zero Interval: Interval between pulses, corresponding to zero voltage input (anode resistor on PMT shorted).

Free-run Interval: Interval between pulses shortly before zero time.

A and B Pulses: Owing to the type of modulator used, it was possible to have two values of interval for the same input voltage—one value between the 1st and 2d, the 3d and 4th, the 5th and 6th, etc., and another value between the 2d and 3d, the 4th and 5th, the 6th and 7th, etc. When the difference between the two intervals is significant, the record is said to exhibit A and B pulses.

Blanking Out: On certain records the PMT current was so high for a period immediately following time zero that the modulator, due inherently to its construction, would fail to produce pulses until the voltage into it was again within range. This phenomenon is termed "blanking out."

Pulse Cancellation: Entirely different from the blanking out defined above is the phe-

TABLE 3.1 EXTENT OF TRANSMITTAL OF INFORMATION TO MAGNETIC TAPE FROM VARIOUS CHANNELS

Particle Energy (Mev)	Electron						Positron					
	Box and Channel No.	Data Obtained?			Error (% full scale)		Box and Channel No.	Data Obtained?			Error (% full scale)	
		Linear Amp Pulses	Modulator Pulses	Preshot Calibration	Preshot Calibration	No Calibration		Linear Amp Pulses	Modulator Pulses	Preshot Calibration	Preshot Calibration	No Calibration
					Station E-57							
0.422	VII-1	Yes	Yes	Yes			VII-6	Yes	Yes	Yes		
0.525	I-6	Yes	Yes	No	6	4	I-1	Yes	Yes	Yes	3	
0.651	VI-6	Yes	Yes	Yes			VI-1	Yes	No			
0.802	II-1	Yes	Yes	Yes			II-6	No	No			
0.982	V-1	Yes	Yes	Yes	9		V-6	Yes	Yes	Yes	6	
1.19	III-6	Yes	Yes	Yes	6		III-1	Yes	Yes	Yes	3	
1.41	VII-2	No	Yes	Yes			VII-5	No	Yes	Yes		
1.45	IV-6	Yes	Yes	Yes	3		IV-1	Yes	Yes	Yes	9	
1.71	I-5	Yes	Yes	Yes	9		I-2	No	Yes	Yes	9	
2.05	VI-5	Yes	No	No			VI-2	Yes	No			
2.46	II-2	Yes	Yes	No	6	4	II-5	Yes	Yes	Yes	9	
2.93	V-2	Yes	Yes	Yes	9		V-5	Yes	Yes	Yes	9	
3.49	III-5	Yes	Yes	Yes	3		III-2	Yes	Yes	Yes	3	
4.04	VII-3	Yes	Yes	Yes			VII-4	Yes	Yes	Yes	6	
4.13	IV-5	Yes	Yes	Yes	3		IV-2	Yes	Yes	No		
4.79	I-4	Yes	Yes	No	6	4	I-3	Yes	Yes	No	6	4
5.66	VI-4	No	No	Yes			VI-3	Yes	Yes	Yes		
6.69	II-3	Yes	Yes	Yes	6		II-4	Yes	Yes	Yes		
7.87	V-3	Yes	Yes	Yes	9		V-4	Yes	Yes	Yes	6	
9.22	III-4	Yes	Yes	Yes			III-3	Yes	Yes	Yes		
10.9	IV-4	Yes	Yes	Yes	3		IV-3	Yes	Yes	Yes	3	
					Station E-54							
0.422	VII-1	Yes	Yes	No	6	10	VII-6	Yes	Yes	No	6	10
0.525	I-1	Yes	Yes	No	6	10	I-6	Yes	Yes	No	6	10
0.651	VI-6	Yes	Yes	No	6	10	VI-1	Yes	Yes	No	6	10
0.802	II-1	No	Yes	No	6	10	II-6	Yes	Yes	No	6	10
0.982	V-6	Yes	No	No	6	10	V-1	Yes	Yes	No	6	10
1.19	III-6	No	Yes	No	6	10	III-1	No	No	No	6	10
1.41	VII-2	Yes	Yes	No	6	10	VII-5	Yes	No	No	6	10
1.45	IV-1	Yes	Yes	No	6	10	IV-6	Yes	Yes	No	6	10
1.71	I-2	Yes	Yes	No	6	10	I-5	Yes	Yes	No	6	10
2.05	VI-5	Yes	Yes	No	6	10	VI-2	Yes	Yes	No	6	10

2.46	II-2	No	Yes	No	6	10	II-5	Yes	Yes	No	6	10
2.93	V-5	Yes	No	No	6	10	V-2	Yes	Yes	No	6	10
3.49	III-5	No	Yes	No	6	10	III-2	Yes	Yes	No	6	10
4.04	VII-3	Yes	Yes	No	6	10	VII-4	No	Yes	No	6	10
4.13	IV-2	No	Yes	No	6	10	IV-5	Yes	No	No	6	10
4.79	I-3	Yes	Yes	No	6	10	I-4	Yes	Yes	No	6	10
5.66	VI-4	Yes	Yes	No	6	10	VI-3	Yes	Yes	No	6	10
6.69	II-3	No	Yes	No	6	10	II-4	No	Yes	No	6	10
7.87	V-4	Yes	Yes	No	6	10	V-3	Yes	Yes	No	6	10
9.22	III-4	Yes	Yes	No	6	10	III-3	No	Yes	No	6	10
10.9	IV-3	Yes	Yes	No	6	10	IV-4	Yes	Yes	No	6	10

Station C-57

0.422	VII-1	No	Yes	VII-6	Yes	Yes	Yes
0.525	I-6	Yes	Yes	I-1	Yes	Yes	Yes
0.651	VI-6	Yes	Yes	VI-1	No	No	Yes
0.802	II-1	Yes	Yes	II-6	No	Yes	Yes
0.982	V-1	No	No	V-1	No	No	Yes
1.19	III-6	Yes	No	III-1	Yes	Yes	Yes
1.41	VII-2	No	Yes	VII-5	Yes	No	Yes
1.45	IV-1	No	Yes	IV-6	No	Yes	Yes
1.71	I-5	No	Yes	I-2	Yes	Yes	No
2.05	VI-5	Yes	No	VI-2	No	Yes	Yes
2.46	II-2	No	Yes	II-5	No	Yes	Yes
2.93	V-2	No	No	V-5	No	No	Yes
3.49	III-5	No	Yes	III-2	No	No	Yes
4.04	VII-3	No	Yes	VII-4	Yes	Yes	Yes
4.13	IV-2	Yes	Yes	IV-5	Yes	Yes	Yes
4.79	I-4	Yes	Yes	I-3	Yes	Yes	Yes
5.66	VI-4	Yes	Yes	VI-3	No	No	Yes
6.69	II-3	Yes	Yes	II-4	Yes	Yes	No
7.87	V-3	Yes	Yes	V-4	Yes	Yes	Yes
9.22	III-4	No	Yes	III-3	Yes	Yes	Yes
10.9	IV-3	Yes	Yes	IV-4	Yes	No	Yes

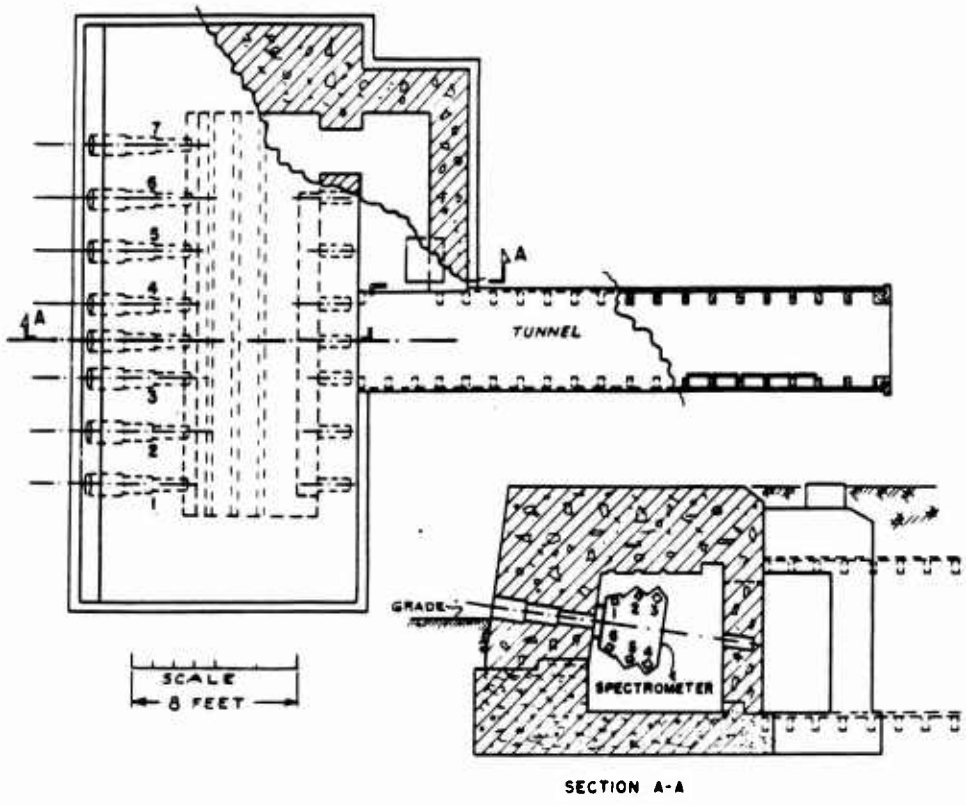

Fig. 3 1 Physical Location of a Given Energy Channel

nomenon which results in the elimination of certain of the pulses. This effect is the result of cross talk from other channels and the reference channel (see Sec. 3.1.3).

Difference Interval: The difference between the zero interval and the free-run interval in microseconds.

Hash: From zero time to 300 to 400 μsec, disturbances on the line create spurious signals, called "hash," which mask the true signal.

The procedure that was followed is illustrated in the block diagram of Fig. 3.2. The details of the procedure were changed periodically to reduce errors and to take advantage of late arriving equipment ordered for the job. Initially, the scheme described in reference 2 was used to change the form of the data from magnetizations on the tape to deflection modulated oscillographs on 35-mm film. A section of a typical record, showing the signal pulses mixed with the marker pulses (which were controlled by the signal generator set to the reference frequency), is shown in Fig. 3.3. The film record was then read on microfilm readers, and the data were recorded in ruled data books. Each film record was first run across a lighted ground glass panel, and the reference markers corresponding most nearly to integral values of milliseconds from zero time were marked. The method of removal of data from the films is best illustrated by reference to a typical data sheet as portrayed in Fig. 3.4. Owing to the phenomenon of pulse cancellation, there are two basic types of pulse intervals to be determined. They are the total interval occupied by a group of successive pulses (which seldom exceed four in number) and the succeeding interval during which one or more pulses had been canceled. In the first column the number of intervals with no apparent missing pulses in the group is listed; intervals of cancellation are denoted by a dash. In the third column the number of full 20-μsec intervals (the basic reference marker interval in the initial system) was put down. The fraction, in tenths, of the last basic interval which transpired before the pulse occurred is recorded in the fourth column. This fraction determines the figure to be entered in the second column, which is the fraction of the basic interval from the signal pulse in question to the next marker pulse. Thus the sum of the entry in column 4 and the entry in column 2 of the next line down equals unity. The fifth column sums the readings in the second, third, and fourth columns. To keep track of the total elapsed time, the millisecond marker, if any, which occurs within the interval is shown in column 6. By multiplication by 20 and division by the number of intervals, the average interval per pulse in the group of pulses is determined.

The job of converting from pulse interval to counts per second requires a chart of voltage developed vs signal interval in microseconds, and a chart of photomultiplier anode current as a function of voltage was developed. If the preshot calibration mechanism functioned properly, the first chart is available for each individual channel from data contained near the beginning of each tape. Intervals can be determined from the tape which correspond to 0, 3, 8, 13, and 18 volts being applied to the modulator. The required function is obtained by plotting these five points and drawing a straight line through them, as shown in Fig. 3.5. The second chart is universal in that it applies to all channels. It is shown as Fig. 3.8 of reference 3. The actual voltages corresponding to given intervals were computed from the zero interval and the slope value which most nearly coincided with the five points obtained from the record, rather than using the less accurate method of picking them from a drawn graph.

3.1.2 Limitation in Precision of Data Due To Reduction of Data and Malfunctions of Equipment

The first error arises from the assumption that the frequency variation of the reference signal during the run was negligible. The first estimate of the variation made from observing the Lissajous figure of the reference wave and the signal generator controlling the reference markers on the film was found to be low, and all channels with significant information were rerun, using a different system. About this time it was also discovered that the basic frequency of the reference signal was not 5000 cycles/sec (on playback at 1/100 of the recording speed) but 1250 cycles/sec. This phenomenon remained undiscovered for so long owing to the fact that the reference track amplifier in the reproducer was tuned sharply to 5000 cycles/sec

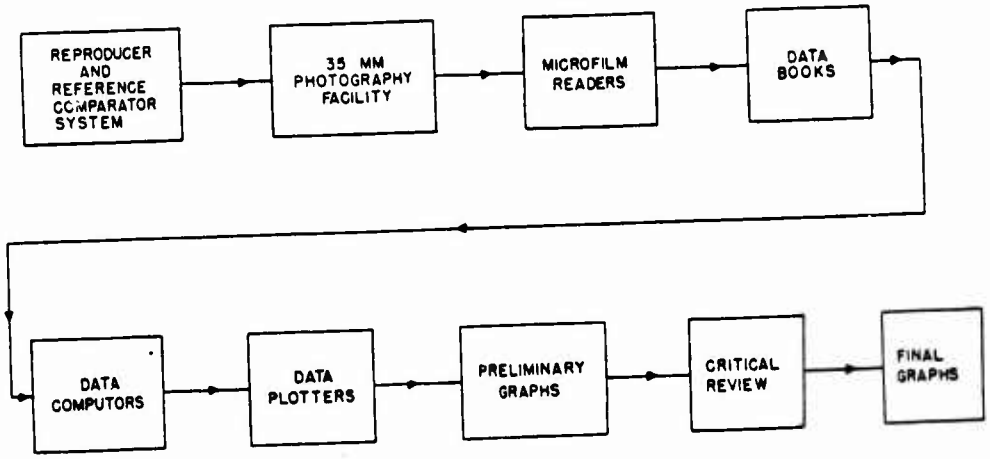

Fig. 3.2 Block Diagram of Data Recovery

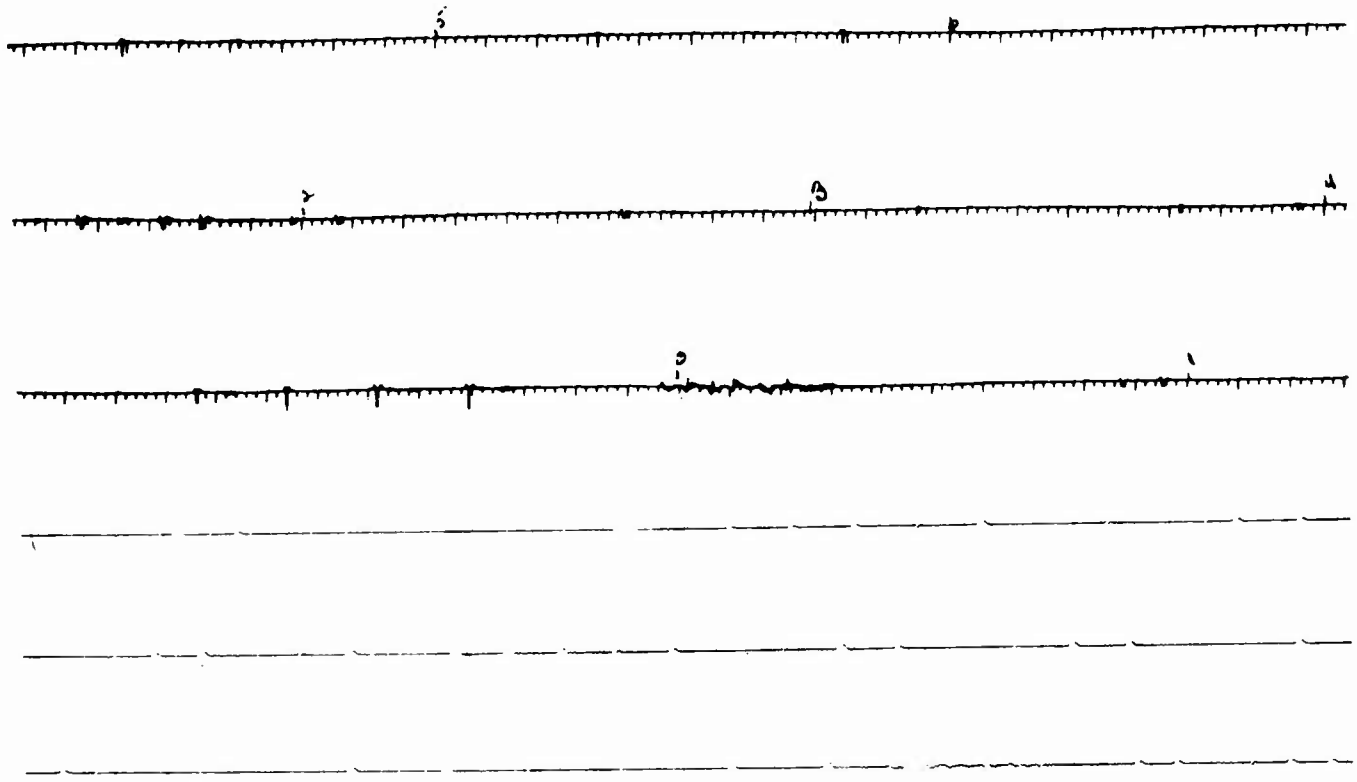

Fig. 3.3 Typical Film Records. Bottom, 16-mm double beam. Top, 35-mm single beam, mixed signal and markers.

E54 X-1 (63H) RECORD

Number of Intervals	First Fraction 20/sec	Full Number 20/sec	Second Fraction 20/sec	Total Time 20/sec	Mid-Second Marker Number	Time Per Pulse 20/sec Intervals	Δτ/pulse μ Sec Intervals	B - Δτ μ sec	$\frac{B-\Delta\tau}{B-A} V_2$ Volts	Output Current Amps	10^6 Counts Per Second	10^3 Photons Per Adv. Per in^2 Per Sec.
Hash	0.	14		14.0								
—		18		18.3								
4	.9	6	.7	7.6		1.90	38.0	146.6	24.4	4420	894	3050
4	.3	6	.7	7.0		1.75	35.0	149.6	24.9	4990	998	3400
1	.3	1	.2	1.5		1.50	30.0	154.6	25.8	7490	1480	5050
—	.8	2	.6	3.4	1	1.70	34.0	150.6	25.1	5310	1042	3553
4	.4	6	.6	7.0		1.75	35.0	149.6	24.9	4990	998	3400
2	.4	3	.3	3.7		1.85	37.0	147.6	24.6	4680	936	3190
1	.7	1	.4	2.1		2.10	42.0	142.6	23.8	3850	770	2630
—	.6	11	.6	12.2								
2	.4	4	.2	4.6		2.30	46.0	138.6	23.1	3100	620	2110
—	.8	17	.5	18.3		3.05	61.0	123.6	20.6	640	128	436
2	.5	5	.6	6.1	2	3.05	61.0	123.6	20.6	640	128	436
1	.4	3	.2	3.6		3.60	72.0	112.6	18.8	383	76.6	261
—	.8	27	.9	28.7		3.60	72.0	112.6	18.8	383	76.6	261
2	.1	8		8.4		4.05	81.0	103.6	17.3	226	45.2	154
2		8	.3	8.3	3	4.15	83.0	101.6	16.9	185	37.0	126
2	.7	7	.7	8.4		4.20	84.0	100.6	16.8	174	34.8	119
—	.3	67	.3	67.6	4	4.50	90.0	94.6	15.8	73.0	14.6	49.8
2	.7	8	.8	9.5		4.75	95.0	89.6	14.9	49.9	9.98	34.0
2	.2	9	.6	9.8		4.90	98.0	86.6	14.4	44.7	8.94	30.5
1	.4	5		5.4	5	5.40	108	76.6	12.8	27.9	5.58	19.0
—		10	.2	10.2		5.10	102	82.6	13.8	38.4	7.68	26.1
2	.8	9	.5	10.3		5.15	103	81.6	13.6	36.3	7.26	24.8
1	.5	4	.3	4.8		4.80	96.0	88.6	14.8	48.9	9.78	33.3
—	7	15	.8	16.5								
1	.2	5	.1	5.3		5.30	106	78.6	13.1	31.0	6.20	21.1

Fig. 3.4 Typical Data Sheet

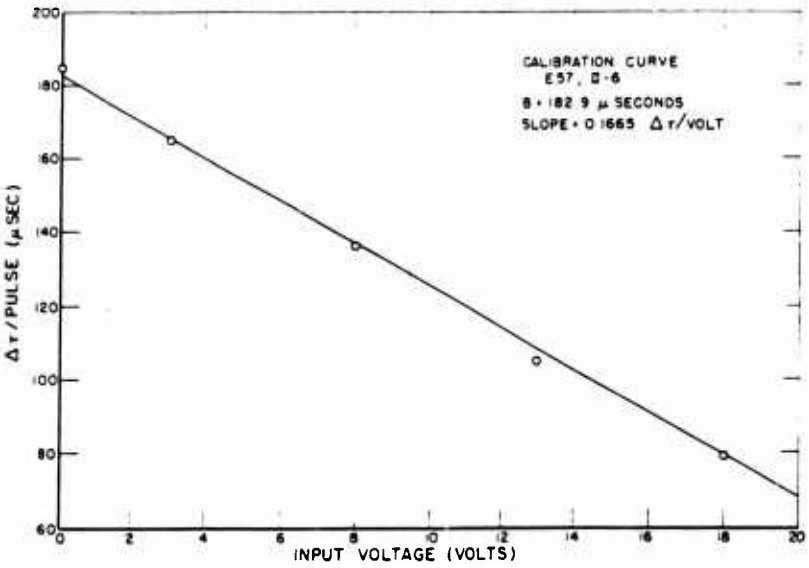

Fig. 3.5 Typical Calibration of Pulse Interval As a Function of Input Voltage

so that its output was actually at that frequency but represented only the fourth harmonic of the true 1250 cycles/sec. Only after the reference track output had been run adventitiously through one of the signal amplifiers whose response was relatively flat in this region did the truth become known. In the improved playback system the 1250-cycle/sec reference frequency and the desired signal were displayed on separate beams of a Du Mont type 279 double-beam oscilloscope. These two deflections were photographed this time on 16-mm film with a moving-film camera capable of driving the film at 36 in./sec. A typical record is shown in lower Fig. 3.3. The true interval was obtainable by counting the number of cycles of the reference frequency between each pulse or group of pulses, regardless of variations of reference frequency due to changes in tape speed during either recording or playback.

A second error was due to the preshot calibration problem. Not all the channels which produced signal pips had a preshot calibration because of the failure of calibrating relays or the failure of the master calibrating system to function. Table 3.1 lists those channels which did have signal pips and those which also had a preshot calibration. If a calibration was available, trouble was sometimes experienced in deciding the proper slope line to be drawn through the five points on the graph. There was actually a sixth point, which corresponded to the voltage obtained with the calibration lead connected to the high impedance input to the modulator but with an open circuit applied to the other end. This voltage has no meaning but was confusing in the case where one of the proper calibration points was missing. The points were in general not exactly in line; therefore considerable judgment had to be exercised in the establishment of the slope. It is estimated that in about 50 per cent of the cases the spread in reasonable slopes that could be obtained was 1 per cent; in the remainder it was 3 per cent.

In the cases where immediate preshot calibration had been lost, the limit of error must necessarily be widened. To obtain the most probable value of slope to use in these cases, the average slope for the calibrated channels at the same station was calculated. The most probable zero interval for each uncalibrated channel is obtained by combining the average difference value from the other channels with the measured free-run interval of the channel. None of the calibrations were available from Station E-54, and the averages from Station E-57 were used. In order to estimate the error involved in the procedure used, the averages of the slopes, difference values, and zero intervals with their standard deviations for each spectrometer station are given in Table 3.2. The same information for the spatial station[4] is given for comparison.

TABLE 3.2 STANDARD DEVIATIONS OF SLOPES, RESIDUAL CURRENTS, AND ZERO POINTS

Station	Difference Interval (μsec)		Slope (volts/μsec)		Zero Point (μsec)	
Spectrometer Stations						
C-57	3.2	0.96	Error in one calibration voltage		198.7	3.3
E-57	3.6	1.27	0.1648	0.0017	182.4	1.9
Spatial Stations						
E-53	5.4	1.19	0.1808	0.0025	186.4	0.9
C-53	2.22	1.86	0.1766	0.0024	192.5	2.1
C-52	Data not used		0.1814	0.0011	189.0	1.3

Short-term errors, which cancel out if several intervals are measured and the average taken, also exist; their primary effect is to increase the resolving time for a given accuracy of measurement. The most serious of these errors is due to the phenomenon of cancellation of pulses. The reasons for the missing pulses are covered in Sec. 3.1.3; their effect on the accuracy of the data will be considered here. The percentage of pulses that were missing spread from 40 to 70 per cent for the spectrometer channels. The pulses had a tendency to be missing in groups, and the average number missing per group was roughly two. The net effect of this error combined with those to be described below was to increase the inherent time resolution of the system from the designed value of 200 μsec to the order of 1 msec.

In order to obtain better accuracy in establishing the basic interval between pulses, a graphical method was used. The time interval between pulses for every pulse seen on the film was recorded, and these values were plotted against time. The result was a series of similar curves, one being a multiple of another. The basic interval was chosen as the lowest curve or the smallest difference between curves. In all cases these values were identical. The higher curves were then divided by the integer that fitted it with the basic curve. This constituted the $\Delta\tau$/pulse vs time curve. Values of $\Delta\tau$/pulse were taken from this curve, computed, and plotted as the final curves of dosage rate vs time. A sample curve of $\Delta\tau$ vs time is shown in Fig. 3.6.

The variability in the pulse heights on playback and the decrease in the frequency of the reference track resulted in an uncertainty of 4 μsec in the determination of an interval. By counting over a sufficient number of intervals and taking an average, the error could be reduced, but, at short times where the interval was changing rapidly, this and the other short-term errors took their toll in reducing the accuracy of the spectrum determination.

The difference in the orientation of the tape between recording and playback will cause short-term errors if this angular difference is varying rapidly with time. A brief computation will show that an angular difference of 0.01° will cause a change of 1 μsec in the relative position of the signal pulse and the reference signal in the worst case, i.e., the head position most remote from the reference head.

The hash that is evident for the first fraction of a millisecond does not contribute an error as such but simply reduces the amount of data that is available. In many cases the limitation in dynamic range of the instrument resulted in blanking out of pulses for a period considerably longer than the hash period, and thus the data lost due to hash were much less than the data lost due to dynamic range limitation.

In estimating the error in the measurement of the counting rate in a channel in order to evaluate the accuracy of a spectrum obtained from relative readings in the various channels, it is necessary to add the short-term errors described above to the inherent long-term errors due to the calibration and the electronics[1] and to the malfunctions of the equipment.

Rather than try to evaluate each short-time error and combine them statistically, it was considered more valuable to estimate the total effect of the short-term errors from the deviations about the mean on portions of the record where the variation in counting rate is known to be slight during several milliseconds.

The error due to the short-term effects can be made as small as necessary by worsening the time resolution. By averaging points over about 1½ msec, it is estimated from the curves that the short-term error can be held to 10 per cent, which must be combined with the errors estimated in reference 1. The error due to the uncertainty of the slope of the line drawn through the calibration points must be included for those units which had precalibration, and, for those which did not, a larger error must be used, depending on whether any of the units at a particular station had calibration or not. Table 3.1 lists the errors for the various spectrometer stations and channels.

3.1.3 Investigation of Recorder Difficulties

The recordings for all units of the project were characterized by cancellation of from 30 to 70 per cent of the pulses in such a fashion that it was apparent that some form of beating of waves of different frequencies was occurring. In addition, it was determined that the reference frequency which was recorded on the tape was 125 kc/sec instead of the designed value of 500 kc/sec. Therefore an investigation was undertaken to determine the causes of this anomalous behavior. A highly significant clue finally led to a reasonable explanation. It was observed on certain double-beam records, displaying the 125-kc/sec reference frequency and a signal pulse record side by side, that the pulses occurred only in a certain phase span of the reference sine wave. This phase span was generally about ½ cycle. This led to the theory that the beating was occurring with one or both of the reference signals rather than with adjacent channel pulses, as had been previously supposed. An experiment was performed to isolate the cancellation process to see if it occurred before or after the blocking oscillator tube. The tape was run at a higher speed on the theory that the missing pulses would appear above the constant background of the reproducer as they were amplified by the higher tape

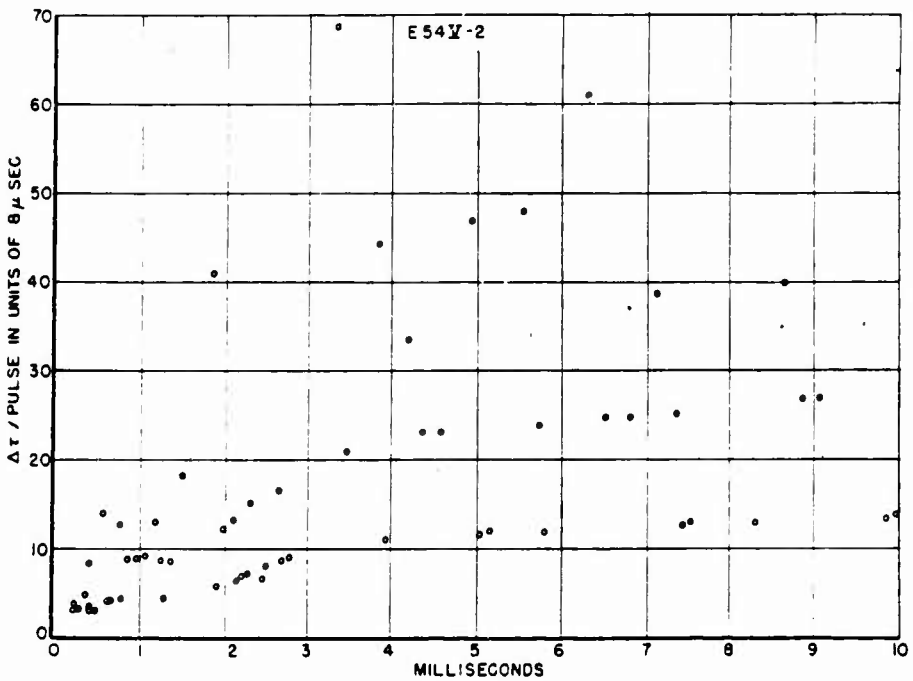

Fig. 3.6 Typical Pulse Interval vs Time Curve

speed if the cancellation occurred after the blocking oscillator. The pulses failed to appear; it was therefore concluded that the blocking oscillator was actually prevented from firing by the cancellation process. Further proof that the cancellation was not interference at the heads was the inability to reproduce sufficient cancellation in the laboratory under any reasonable ratio of driving voltages and the fact that the cancellation was independent of the position of the signal head with respect to the reference head.

The only factors common to the reference and the signal circuits were the heater voltages and the plate supply voltage. However, the heater voltages are quite unlikely as a source of trouble due to the fact that they are common to only two recorders; all indications are that the culprit was common to the whole recorder shelter. The effect could be explained in terms of feed-through of reference voltage on to the blocking oscillator circuit so that the reference voltage would prevent triggering of the blocking oscillator during a certain portion of its cycle. A common 100-ohm impedance was inserted in the B^+ lead of one recorder, and an effect very similar to that observed on the shot records was obtained with a large (100-ma peak) drive on the reference head at 100 kc/sec.

The appearance of 125 kc/sec as the reference signal is not so easily explained. It has been verified by a simple Lissajous figure experiment that the two reference signals remain in phase over a period of 1 or 2 min. It is highly unlikely that two crystals are able to stabilize frequency to this extent, and it must be concluded that one head was driving the other. With the 100-ohm common impedance it was possible to swamp completely the internal 500-kc/sec reference signal with feed-through from the external reference signal of 100 kc/sec and of sufficient amplitude to give a response on the tape comparable to that obtained on the shot records. It is highly probable that the external reference generator was affected by the common impedance or, for some other reason, oscillated at one-fourth the crystal frequency with sufficient amplitude to cause the effects noted. Unfortunately, the master control panel containing the external reference generator which was used in the field was sent to Los Alamos and was therefore not available for rechecking.

3.1.4 Performance of Recorder and Playback Equipment

Considerable difficulty was experienced at preshot time due to the 400 volts used for B^+. Tuning eye tubes blew up, 6AG7 tubes developed shorts to ground, and 500-kc/sec crystals burned out. It was found that reducing the plate voltage to 360 volts alleviated the situation, although considerable trouble was still experienced with 6V6 tubes in the oscillator circuit, due in part to the inferior grade of tubes which had to be taken to get a sufficient quantity in time. The drive mechanisms ran very reliably throughout the preshot tests, provided that they were adjusted properly. No head failures were noted during this period. The master control system performed through all dry runs without incident.

The major problem in regard to the recordings throughout the operation was the heat phenomenon which existed when large numbers of signals were fed simultaneously to the recorder banks. This effect was noted first from the results of Dog shot. Attempts were made to correct this difficulty by not feeding pulses with large differences in amplitudes to the same recorder. It was found that the pulses from Stations 54 and 57 were in general 60 to 80 per cent greater than the pulses from Stations 52 and 53. On Easy shot it was arranged that no spectrometer cables were fed to recorders that had spatial channels, and on the dry run, with 80 per cent of the channels feeding pulses, the effect appeared to be mitigated. However, on the actual run, with all channels feeding pulses, the periodic blocking of pulses was universal. On George shot every other channel was used, and the channels were duplicated on a second 24-channel recorder. This proved to be a valuable safeguard as the tape broke on the duplicate recorder. This was the first such failure on all the test and dry runs and was attributed to setting the tape tension too tightly in an attempt to reduce flapping of the tape. The modulation was much less on these few channels, except for one signal which had no modulation up to zero time and then varied violently in amplitude to shock arrival. The skipping of pulses which was evident on the first two shots was not catastrophic for it was, in general, possible to obtain an accurate reading at least every millisecond, which was the time resolution which was required initially.

Some time after playback of the tapes for data recovery was underway, it was discovered that all recorders had time reference tracks which were recorded at 125 kc/sec instead of the designed value of 500 kc/sec. This submultiplication of both the internal and external reference frequencies has never been satisfactorily explained. Attempts to duplicate the results using the same recorders at the Bureau of Standards Laboratory by changing supply voltages to the units were to no avail. The change in reference frequency was not serious as long as the ratio of 4 to 1 between the crystal frequency and the recorded frequency was maintained, which was evidenced by the synchronization between the internal and external recorded frequencies. If there were no relation between these frequencies and their corresponding crystal frequencies, their difference frequency would vary widely with time; this was not the case.

An experiment was performed to try to determine the cause of the cancellation of pulses on the signal channels. A four-channel pulse generator was built, and pulses slightly different in frequency were fed to a cluster of heads in close proximity. There was noted a modulation of 10 per cent at most on any of the signals. This bore out the observation in the field that the effect was not pronounced until all the channels were feeding the recorders. Further evidence that the difficulty was not tape, head, or pulse circuit cross talk was the appearance of modulation on the signal in the sole functioning channel of the four-channel recorder for the 50B control tube output on C site. Also the modulation on adjacent channels appears unrelated, as shown in Fig. 3.3.

3.1.5 Effect of Condenser Coupling of Anode of Photomultiplier to Count Circuit in Spectrometer Electronics

A computation of the expected counting rate in a channel of the spectrometer, made by assuming a spectrum flat in intensity from 0.5 to 8.0 Mev and using the data on gamma rays vs time made available from previous tests, indicated that at short times (approximately 1 msec) at least some of the channels would be reading low in the first decade of the integrating circuit. From data given by King,[5] a 40-kt bomb measured 5.4×10^{25} gammas/sec at 100 μsec (this value was about a factor of 10 higher than expected, according to King). The attenuation factor at 750 yd for 4-Mev radiation is about 0.07. The inverse square at this distance was 1.09×10^{-10} in.$^{-2}$. Assuming that the fission fragments were distributed uniformly in a sphere and that the radius of this sphere was the same as the radius of the ball of fire at short times, the fraction of the source seen by the spectrometer foil at 1.0 msec was about 7.6×10^{-3}. Of the total number of gamma rays present, with a spectrum as assumed above, the fraction that would be effective in any given channel is approximately 0.05. The fraction of the total number of photons effective in any channel, then, was expected to be not larger than the product of the above factors, namely, 2.9×10^{-15} per sq in.

The photon rate effective in any given channel at 1 msec was expected to be not greater than $5.4 \times 10^{25} \times 2.9 \times 10^{-15} = 1.6 \times 10^{11}$/sec. The efficiency of conversion of photons to counts in a channel varies from about 1.3×10^6 photons/count at a gamma-ray energy of 0.615 Mev to about 1.9×10^4 photons/count at 11.1 Mev. The counting rate for these two cases would be 1.2×10^5 and 8.4×10^6 counts/sec, respectively. These values correspond to 5.6 and 14.2 volts across the integrator. The lower value was expected to be even lower than the above computation because of the greater gamma-ray attenuation between source and detector, and the higher value was expected to be a little higher because of less attenuation of the gamma rays.

The lower limit of the integrator was fixed at 10^5 counts/sec at the top of the lowest decade by considering the largest charge per pulse practical while maintaining a satisfactory signal-to-noise ratio and the largest practical resistor for the R-C combination in the lowest decade. It is apparent that individual counts had to be recorded if data were to be obtained in the lower intensity channels.

To achieve this a count circuit was added to the PMT anode. This circuit was coupled to the anode by means of an R-C combination having a charging time constant of 5.6 msec. The discharge time constant of this combination depended on what decade of the integrator was functioning at the time in question. The recovery time of the recorder was the feature that limited the rate at which individual electrons could be counted. It was such that, at a

rate of 2×10^4 counts/sec, about 90 per cent of the counts would be recorded.

The coupling network proved to be an unfortunate addition to the circuit. The data indicated a much higher intensity, particularly in the low-energy channels, than had been anticipated. This high intensity charged the condenser in the coupling network so that after a few milliseconds, when the intensity was lower because of the smaller fraction of the source seen, the discharge of this condenser combined with the PMT output to give an incorrect reading. In fact, after several milliseconds, the record follows very closely just what would be expected from condenser discharge, indicating that the PMT contribution at this time is small.

The discharge time constants are approximately as follows: 1st decade, 106 msec; 2d decade, 15.6 msec; and 3d decade, 6.6 msec. Figure 3.7 is a graph of a typical set of data which clearly shows the effect of condenser discharge. The points at which the integrating circuit switched decades are indicated. This figure may be compared with Fig. 3.8, which is a graph of laboratory data of integrator current as a function of time when the charged condenser is the only current source. The condenser was charged to 22.5 volts, and time was measured from the instant at which the battery connection to the condenser was broken. The contribution of the condenser after about 5 msec is obvious in Fig. 3.7.

Because of this circumstance, data from the integrating circuit could be considered only for the time interval 0 to about 5 msec. An additional difficulty arose as a result of the R-C network being in parallel with the log circuit. Until the charge on the condenser was sufficient to cause a voltage across the condenser equal to that across the log circuit, the coupling network acted as a shunt to the log circuit. The effect of this shunt for a given charge on the condenser was, of course, greatest when the lowest intensity decade of the log circuit was the one functioning and progressively less for the higher decades. The data used for computing spectrum were taken at a time when the voltage across the condenser was almost as large as the voltage across the integrator, in which case the shunting effect was small.

Data from the counting circuit could be considered valid only after two conditions were satisfied. First, the counting rate had to be low enough so that few counts were being lost because of the resolving time of the recorder. Second, the charged coupling condenser had to have discharged enough so that the discharge current did not seriously affect the input to the counting circuit.

The above requirements were met in Station E-57 at about 300 msec. Station E-54 did not satisfy the requirements during the life of the record. A spectrum analysis was then attempted at 3 msec on both Stations E-54 and E-57 and at 300 msec on Station E-57.

3.2 ANALYSIS AND INTERPRETATION OF DATA

The data recorded from each spectrometer energy channel were expressed finally in terms of the counting rate of the detector as a function of the time elapsed from zero time. The method used to record the data in this final form is explained in Sec. 3.1, and the curves obtained from the converted data are shown in Figs. 3.9 to 3.12. It is necessary next to analyze these data for the purpose of determining the gamma-ray spectra at certain specified times.

3.2.1 Selection of Times for Determination of Spectra

It was the initial purpose of this experiment to determine the spectrum at various times in the interval during which the detecting equipment could be expected to function reliably. However, because of the limitations of the data as discussed in Sec. 3.1, it was necessary to exclude from consideration a large part of the useful time interval. In particular the time interval after about 5 msec in the case of the integrating channels[6] was excluded because of the condenser discharge effects. In addition, the blanking-out effect (Sec. 3.1.2) of the detecting equipment at early times made the data less reliable as the time approached zero time. Also the time interval before about 200 msec was excluded in the case of the count channels because of the saturation in the counting rate produced by the high intensities.

From a careful evaluation of the data shown in Figs. 3.9 to 3.12, it was decided that the times at which the data could be most accurately interpreted were as follows:

(Text continues on page 62.)

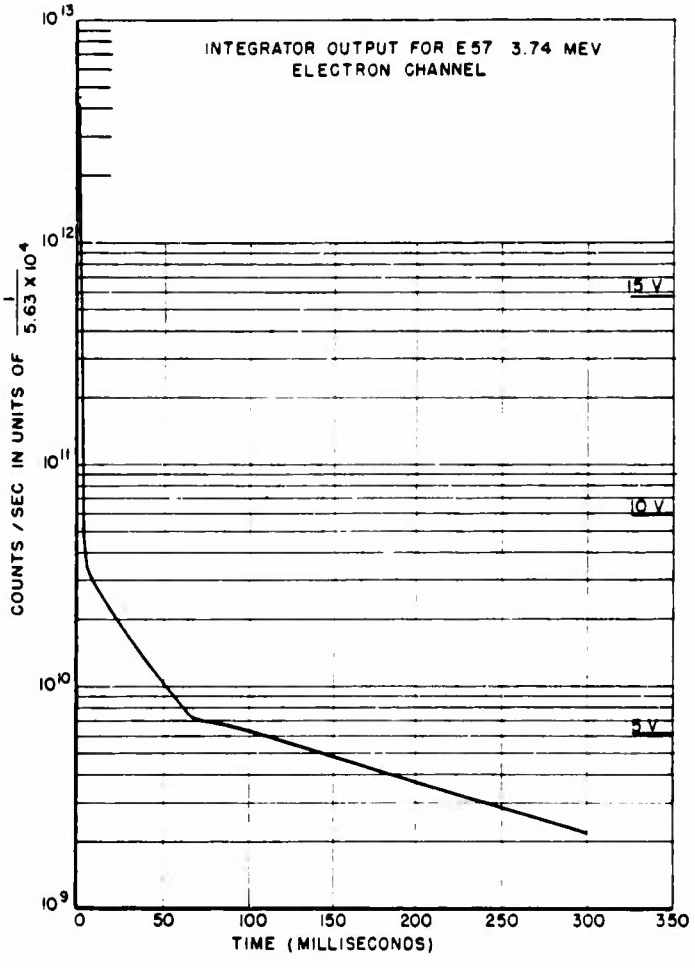

Fig. 3.7 Integrator Current When Source of Current Is PMT and Charged Condenser

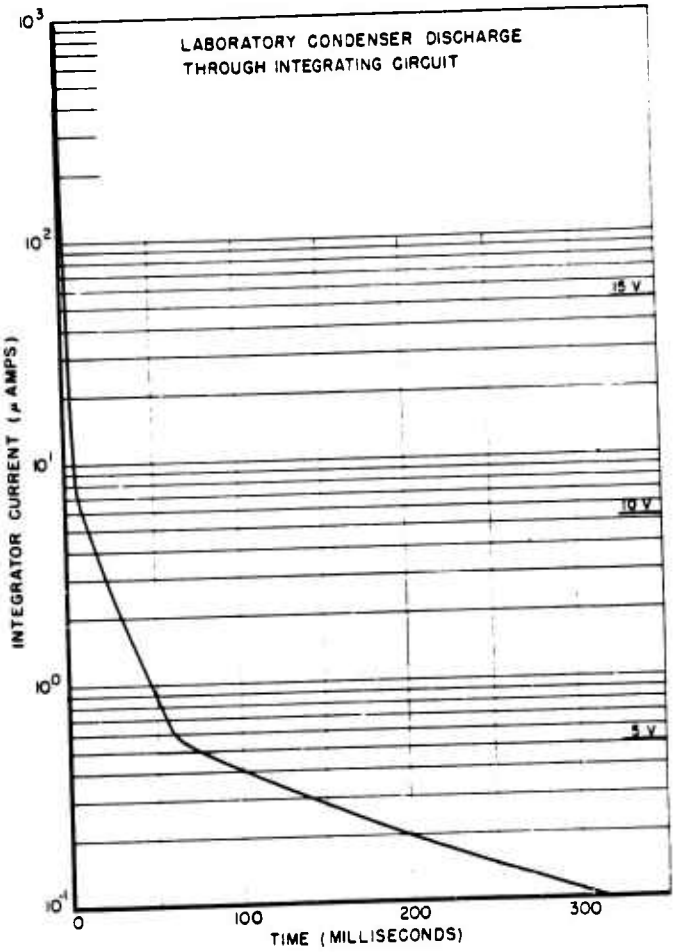

Fig. 3.8 Integrator Current When Source Is Charged Condenser Only

Page 44 - 61 deleted.

Station	Time (msec)
E-57	3
E-54	3
E-57	300

The data on Site C proved to be insufficient to permit any determination of the spectrum. Therefore the problem is reduced to the determination of the spectra on Site E at the three specified times.

3.2.2 Determination of Compton Electron Counting Rates

The PMT current in a given spectrometer channel arises as a consequence of the scintillations in the PMT crystal produced by one or more of the following three possible sources:

1. Electrons ejected from the beryllium foil in the spectrometer.
2. Positrons ejected from the beryllium foil in the spectrometer.
3. Background radiation.

The background radiation (3) consists primarily of scattered gamma rays, gamma rays from captured neutrons, and electrons. At a given time the charging rates (I^- and I^+, respectively) recorded for a particular electron channel and for the corresponding positron channel can be expressed as

$$\begin{aligned} I^+ &= I_B^+ + I_{\beta^+} \quad \text{positron channel} \\ I^- &= I_B^- + I_C + I_{\beta^-} \quad \text{electron channel} \end{aligned} \tag{3.1}$$

where I_B^+ and I_B^- = charging rates due to background radiation

I_{β^+} = charging rate due to positrons from the foil

I_{β^-} = charging rate due to pair-production negatrons from the foil

I_C = charging rate due to Compton electrons from the foil

The conversion to absolute photon intensities is based only on the quantity[7] I_C. In order to determine the quantity I_C, it is necessary to analyze the measured quantities I^+ and I^-. It was initially intended in the planning of the experiment that the quantity I_C could be simply expressed from Eq. 3.1 as

$$I_C = I^- - I^+ \tag{3.2}$$

However, Eq. 3.2 is based on the following assumptions:

1. The electronic detecting system for each PMT head[6] is correctly calibrated so that a given radiation flux incident on a crystal detector would produce the same measured charging rate regardless of which PMT head is used.
2. In Eq. 3.1, $I_{\beta^+} = I_{\beta^-}$.
3. In Eq. 3.1, $I_B^+ = I_B^-$.

The validity of the above assumptions must be established before it is possible to deduce the gamma-ray spectrum.

In the case of assumption 1, if there is a most probable error of P per cent for a given PMT head, then to find the charging rate I_0 that would be produced by a PMT that is correctly calibrated, the measured charging rates I^+ and I^- in Eq. 3.1 must be written as

$$I^+ = I_0^+ \pm \frac{P}{100} I_0^+ \tag{3.3}$$

that is

$$I_0^+ = \frac{I^+}{1 \pm (P/100)}$$

and similarly for I_0^-.

Assumption 2 has been discussed in Sec. 2.5 and is a consequence of the Bethe-Heitler theory that, in the pair-production process, the cross section is symmetrical with respect to the positron and electron. In addition, the evidence from the pile spectrum[8] indicates that the counting rate I_β^- of the pair-production electrons will not contribute more than about 5 per cent to the counting rate of the Compton electrons ($I_{\beta^-} \leq 0.05\ I_C$) and furthermore the counting rates I_{B^-} and I_{B^+} will become negligible in the high-energy channels (above 6 Mev). The fact that the counting rates in the positron channels tend to increase rather than decrease above 6 Mev (see Table 3.3) suggests that the dominant contribution to the counting rates in the positron channels is made by background radiation. It is to be noted further that the high-energy channels which show such high

backgrounds are channels 3 and 4 in each spectrometer (see Fig. 3.1 and Table 3.4).

The data present evidence that assumption 3 which states that the background charging rate I_B is the same in opposite electron-positron channels is not justified in some cases. For example, Figs. 3.9 to 3.12 show cases where the counting rate in the positron channel is actually larger than that in the corresponding electron channel. From Eq. 3.1 the cause of this anomaly must be ascribed to the difference in background counting rates of the positron and electron channels, providing that extreme variations from the calibrated standards have not occurred in the electronic detecting systems of the respective channels. The positions of the spectrometers and energy channels in which the above examples occur are significant.

Station	Spectrometer Position*	Electron Channel and Position*	Positron Channel Position
E-57	3	4	3
E-57	4	4	3

*These positions are identified in Fig. 3.1.

(No data were available from both channels 3 and 4 in spectrometer positions 6 and 7 at Station E-57 and spectrometer positions 3, 4, 5, and 7 at Station E-54. In position 5 at Station E-57, channel 3 which was an electron channel had a higher counting rate than that in the positron channel 4.)

The conclusions reached from these data are:

1. The background in the region of the tunnel and door of the shelter is higher than that at the opposite end of the shelter (see Fig. 3.1).
2. Channels 3 and 4 which are most exposed and have the least protection from background radiation incident on the back sides of the spectrometers (see Fig. 3.1) have higher counting rates than channels 1 and 6.
3. There is an asymmetry in backgrounds for corresponding electron and positron channels, which is most serious for channels 3 and 4.

The above conditions may be recognized more clearly in Fig. 3.13 which shows the variation in the counting rate of the positron channels as a function of the position of the spectrometer and the channel. In addition to this nonuniformity of background among channels, the accuracy of determining gamma-ray intensities is further limited in some channels by the relatively low counting rates above background of the Compton electrons from the spectrometer foil.

Because of the background conditions described above, the following procedure was adopted to determine the quantity I_C (Eq. 3.1).

1. Low-energy channels 1 and 6 for spectrometer positions 1 to 6 and channels 2 and 5 for spectrometer positions 1 and 2 were assumed to have about the same background, and corresponding positron-electron channels were subtracted from each other. [The channels for the spectrometer in position 7 were not included because even for these channels the background variation was large (see Fig. 3.13).]
2. Where there were sufficient data available for some of the high-energy electron channels in positions 2 to 5, the contribution of the positron counting rate I_{B^+} was assumed to be small, and the background of each electron channel was assumed to be about the same as recorded by an adjacent positron channel on the same vertical height of the shelter as the electron channel.

A complete tabulation of the pairing of various energy channels according to the above procedure is shown in Tables 3.3 to 3.11. These tables contain all the data used to evaluate the spectra for the three selected cases. The counting rate I_C was found from Eq. 3.2, and the most probable error for this quantity was found by combining the most probable errors of the paired channels. No attempt was made to estimate the error caused by the background asymmetry. After the counting rate I_C for a given energy channel was determined, the conversion to absolute photon intensities was made by the method discussed in reference 7. The conversion constants by which the counting rate was multiplied to obtain photon intensities were found from Table 5.3 of reference 7. In the case of certain channels at Station E-54, the transmission was reduced by a factor of 10 by slits that were placed over the crystal detector. For these cases the proper correction

(Text continues on page 74.)

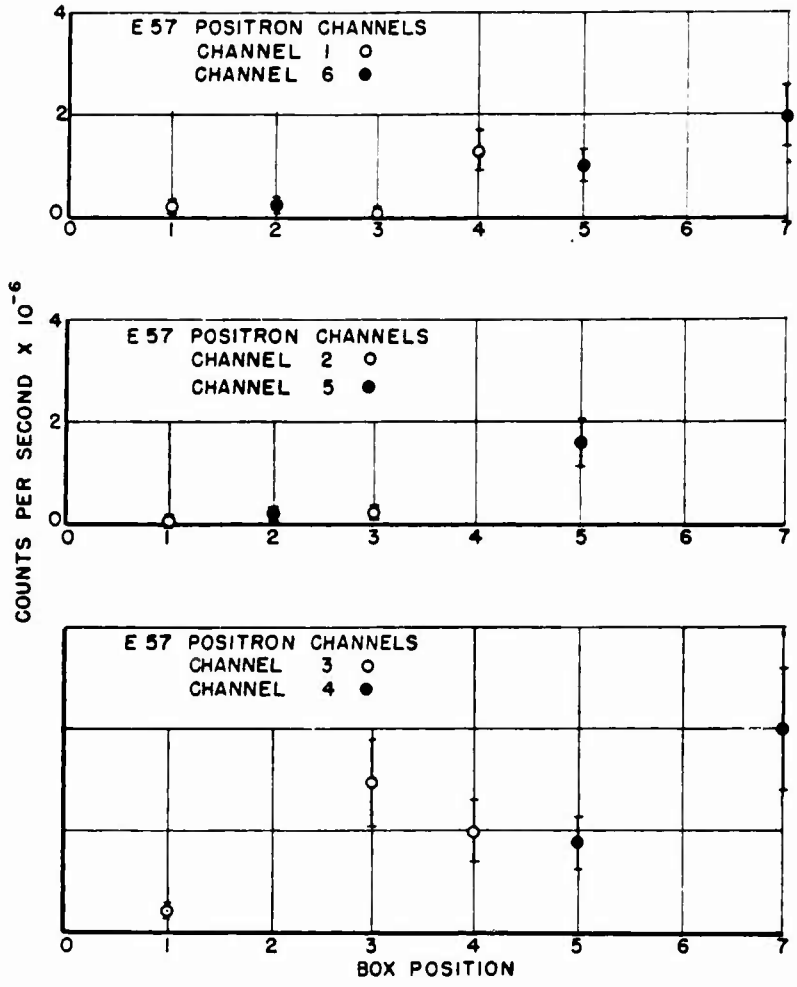

Fig. 3.13 Variation in the Counting Rate of the Positron Channels As a Function of Position of Spectrometer and Channel

Page 65 - 73 deleted.

was made in the conversion constants.

3.3 GAMMA-RAY SPECTRA

The gamma-ray spectra obtained from the data are shown in Figs. 3.14 to 3.16 for the three specified cases: Station E-57 at 3 msec, Station E-57 at 300 msec, and Station E-54 at 3 msec, respectively. Any interpretation of these spectra must allow for the limitations of the data as discussed in the previous section.

In an attempt to check the validity of the data, the Station E-54 spectrum was modified to have the same attenuation and field of view that were obtained at Station E-57. For this comparison it was assumed that the diameter of the source was 50 yd at 3 msec, and standard (narrow-beam) air absorption coefficients were used. This "corrected" spectrum of Station E-54 is compared with the Station E-57 spectrum in Fig. 3.17. The results indicate that the corrected Station E-54 spectrum is about a factor of 10 too high.

The Station E-57 spectrum may also be compared with the pile spectrum,[9] with the understanding that a difference in the shapes of the two spectra would arise because the prompt gamma rays and the gamma rays emitted after about 400 msec are included in the pile spectrum and not in the Station E-57 spectrum. For this comparison the pile spectrum is modified to account for the attenuation produced by 750 yd of air, where the first 60 yd of air has been compressed into a shell by the shock wave at 3 msec. The two spectra are shown in Fig. 3.18, where the pile spectrum has been arbitrarily normalized to match the Station E-57 spectrum at 3 Mev.

A further check on the limits of error between the various measurements may be made by converting the energy flux as a function of photon energy that is given by the Station E-57 and Station E-54 spectra to an integrated dosage rate which can be compared with the dosage rate found from the IvT measurements. In the present case the Station E-50C (1300 yd) IvT dosage rate at 3 msec was used since it was most reliable and since no calibration had been obtained for the Station E-57 IvT data.

The value of the Station E-50C dosage rate at 3 msec is given in reference 9 as 10^4 r/sec. In order to compare the Station E-54 and Station E-57 measurements with this value, it is necessary to make some modifications. First, the total number of photons for each station is corrected for the difference in field of view that is obtained with 2π geometry as compared with the narrow-beam geometry given by the collimator. Then the intensity that would be obtained at 1300 yd is found from the inverse-square law; next, the energy spectrum is modified to account for the difference in air absorption and build-up factor.[10] Finally, the energy flux as a function of photon energy is converted to roentgens with the conversion values given by Mayneord.[11] The total dosage rate obtained is shown in Table 3.12 for the various cases and assumptions made. It is seen that the best agreement is obtained from the Station E-54 energy flux values with the assumption that the source activity is distributed in a shell. The disagreement for all the other cases is not more than a factor of 10.

TABLE 3.12 DOSAGE RATES COMPUTED FROM STATION E-54 AND STATION E-57 SPECTRA

* This value is obtained if, in making the field-of-view correction, it is assumed that the activity is uniformly distributed in the source.

† This value is obtained if it is assumed that the source activity has a shell distribution.

3.4 RECOMMENDATIONS

3.4.1 General Recommendations

The problems involved in making spectral measurements of the type described in this report might be grouped into the following three classes: (1) protection for spectrometers, (2)

Page 75 - 79 deleted.

spectrometer, and (3) detection equipment, i.e., scintillating crystals, phototubes, amplifiers, recorders, etc.

(1) Protection for Spectrometers. Since it is necessary to worry about neutron-induced gamma background as well as background from gamma rays from the bomb itself, the complete problem is rather difficult to handle. WT-107(Ref.) contains a theoretical estimate of the gamma background to be expected behind a 6-ft wall of the limonite aggregate; this estimate pertains to gamma rays from the bomb only. However, analysis of the results as given in this chapter seems to indicate that the major source of the background trouble might well be due to neutron-induced background. If this is true, more care would be required in shielding the back walls of the spectrometer, but the whole problem could be readily resolved by a set of very inexpensive measurements if the existing spectrometer shelters on Runit and Engebi are suitably located with respect to zero points of future bomb explosions. For example, a set of film badges might be distributed throughout the hut on one shot and also on the next shot with a covering of a few inches of boron sand over the outside of the entire hut. The difference would represent the slow-neutron-induced background. In addition, the inside wall could be lined with a boron compound. The resulting data, the integrated dose due to gamma penetration and neutron-induced gammas, would have to be combined with the appropriate IvT information for neutrons and gammas to get the corresponding dose rates at time of the order of 1 msec.

(2) Spectrometer. It appears at present that the Compton spectrometer itself is quite adequate for measurements in the energy range 0.5 to 10 Mev.

(3) Detection Equipment. If future measurements also require time resolution of the order of 1 msec, this will necessarily result in rather complex electronic equipment. Since a large number of channels is required, a large amount of money is risked on a one-shot experiment. It would probably be prudent to build one or two channels, try them out at one set of bomb tests, and if they are successful use them on a subsequent set of tests.

The electronic design philosophy followed on this project was to make the circuits as simple as possible, at the expense of complex calibration equipment and procedures. After the experience in the field, it is recommended strongly that the overriding philosophy should be the following: Cut to the bare minimum the work required in the field even if it requires three times the work in the laboratory. On this basis, then, the circuitry should be complicated to the point of requiring little equipment and time for calibration. The only standard which appeared to have consistent significance in the field was the standard cell, and therefore the ideal calibration for the electronics would depend solely on this type of standard. Power supplies should be made up in the States, and all items should be hooked up and tested prior to being shipped. All items required for a particular measurement on a particular site should be shipped together so that they will arrive simultaneously. Boxes should be sorted out by island prior to shipment, and appropriate color coding should be made. Equipment designations should be marked on the outside of the box, in addition to packing slips, etc.

The concept of precalibration worked very well, as far as it went. In some cases the calibration was not obtained, due mainly to the failure of the calibrating relay on the units to close or to malfunction of the stepping relay calibrating unit itself. It would have been advantageous to have extended the calibration to include the pseudo-log circuit or even the photomultiplier by using a small light controlled by a standard cell. In principle the more precalibrations that are made, the greater is the reliance on the data. In keeping with the principle stated above, very few, if any, controls should be incorporated, accepting differences in the calibrations between units. The transfer functions are obtainable from the precalibration data, and, although the reduction of the data is more complicated, time in the field is again traded for time in the laboratory.

In order to keep the calibrations from being so far out that malfunctions are not readily detectable, the components in the critical circuits should be precision type, and temperature compensation should be used wherever possible. The design should make the calibration relatively independent of supply potentials.

In theory the operation in the field should consist only in these tasks at each measurement site:

1. Assemble pertinent crates, open them, install units and auxiliary equipment ac-

cording to prearranged plan, fasten interconnecting cables, and make functional test.
2. Make radiation calibration, make private dry run of electrical calibration, and check records.
3. Make standard dry run, check records, and make D-1 operational check.

All planning and design should strive for a rapid and simple carrying through of these tasks. For instance, in shipping electronics items, the units can be consolidated in large enclosed racks which can serve a second role of inner box. The outer box could be made with hinges and hasps on the lid, thus saving many man-hours in the field with a small extra expenditure of money. Very close liaison with the construction contractors should be kept in order to ensure that the units will fit in their proper places in the field. The recording shelter should have a portable annex for playing back records in items 2 and 3 above. It should be possible to make the last-minute operational check of each installation in a matter of minutes with a light compact unit containing the necessary test equipment. It is mandatory that the procedures to be followed for the performance of the above task be worked out and practiced on a lifelike mock-up many months prior to going into the field. A preliminary outline should in fact precede any design work on the equipment whatsoever.

3.4.2 Recommendations for Future Tests, Electronics

(1) Intensity Vs Time. The main difficulties encountered with IvT measurements were:

1. Calibration of low-sensitivity detectors.
2. Fatigue of photomultipliers.
3. Complexity of circuit.
4. Low ratio of detector to photomultiplier sensitivity in a uniform gamma-radiation field.
5. Relay failure.

The maximum source size that can feasibly be employed in the field gave a radiation rate at the crystal equivalent to a uniform radiation dosage rate of approximately 13 r/sec. As the maximum dosage rate expected at the near station was between 10^5 and 10^6 r/sec, considerable extrapolation must take place to calibrate the high-level detectors. The use of light for this purpose is complicated by the variation in spectral response of production photomultiplier tubes. Unless the light is nearly monochromatic near the peak of the average spectral sensitivity curve, serious error may result from using a light source with a spectrum broad compared to the sensitive band of the photomultiplier. It is recommended, therefore, that another means of extrapolation be evolved which does not have this difficulty or that a monochromatic light source be used.

Fatigue, even at the 10-μa level, was sufficiently bothersome to reduce the accuracy of a sensitivity determination to the order of 5 per cent. It has been learned since[12] that it is possible to select tubes which have negligible fatigue at the 10-μa level. It was found that the tubes which fatigued worst were in general the most sensitive, and, since the most sensitive were selected for the higher sensitivity positions, fatigue was encountered at these crucial stages. However, it is recommended that in the future the photomultipliers be tested for their fatigue characteristics so that calibrations can be carried out more accurately.

The switching circuitry was conceived and developed at the time that it was considered that recording channels with the accuracy and time resolution required would be at a premium. With the availability of magnetic recording, the cost of a 5 per cent channel was the same as the cost of a 1 per cent channel, and therefore it would have been better to use five different detectors, each with its separate modulator and recording channel. These detectors could be calibrated to have sensitivities which varied by factors of 10 to cover a 10^5 to 1 dynamic range with an accuracy of 1 per cent of full scale of each decade. It is recommended that such a system be considered if the same measurements are to be attempted on a future test.

In the future it is recommended that no light piping be used so that maximum optical coupling is obtained between the scintillation material and phototube. This implies the use of a head-on tube of the 5819 type and a large ampoule of liquid scintillating material in direct contact. The scattering from the phototube should be negligible compared to this much larger contribution from the nonenergy-dependent scintillation material. The much

greater sensitivity so obtained would allow reduced voltages applied to the apparatus, thereby reducing the probability of arc-over due to ionization in the air from the radiation. The leads to the photomultiplier should be radiation shielded to as large an extent as possible without introducing serious scattering errors.

It is recommended that future IvT installations be enlarged to accommodate all electronic equipment and associated power supplies below ground with sufficient shielding to prevent trouble due to radiation ionization. If a large enough hole is provided to permit working in a sitting down position inside the shelter and a trap-door entrance is provided at the back so that special equipment is not required to close up the installation, many of the difficulties encountered on this test could be avoided. The battery rack and relay installation should use hermetically sealed units to overcome failures of relays and switches due to dust particles. Some of the failures of IvT and spatial unit calibrations were due to Potter & Brumfield SM5DG miniature relays. These relays should be avoided.

(2) Spatial Distribution Vs Time. The spatial electronics suffered from insufficient shielding of the power and switching equipment. If this kind of measurement is done again, it is recommended that the concrete block be enclosed to accommodate the ancillary equipment. The forward wall would shield from the direct radiation, and just a small thickness at the sides and back would reduce the secondary radiation to a value which would not affect electronic components. This incidentally would eliminate errors due to ground capture gammas entering the back of the collimator. The calibration system was apparently not sufficiently reliable, and it is recommended that some means of making the calibration more foolproof, such as duplication, be used.

(3) Spectral Distribution Vs Time. The main fault found with the spectrometer electronics was biting off more than could be properly digested. Had there been time for intensive testing of the units, both individually and as a system, prior to production runs, the apparatus would have stood a better chance for success. From the intensity levels observed in this test, it is now possible to predict, at least within a factor of 50, what the intensity at a given time past +1 msec will be, and therefore the complexity required for a large dynamic range becomes unnecessary. The working conditions inside the spectrometer shelter were nearly intolerable. It is recommended that a more efficient ventilation system be devised in future installations. The general recommendations concerning maximum prefabrication for installation and reduction of complexity of calibrations apply particularly here because of the vast amount of circuitry involved.

(4) Recorder Recommendations. If the same magnetic recorders are used again in a future test, time should be allowed for a complete dry run in the laboratory to determine the cause of the cancellation of pulses and to remedy it. Minor changes to the recorders should include current limiting resistors from B^+ to the blocking oscillator tube, fuses local to the recorders, and input volume controls for each channel. A more reliable tube should be substituted for the 6V6 in the crystal oscillator circuits. More ventilation should be provided for the recorder shelter because of fumes from charging batteries. In any future test, provision should be made for the immediate rerecording of data on duplicate tapes or on film to be kept in case of mishap to the primary tapes. The crystal frequency should be reduced to within the range 125 to 250 kc/sec.

Other modifications should be made to the recorders. The reference frequency amplifier should have a flat response from +10 to −10 per cent of the nominal reduced reference frequency and should fall off sharply on either side of the pass band. The amplifier should be redesigned for no tendency to oscillation and for lower noise and hum originating in the input circuits. The input circuits of the signal amplifiers should also be modified for lower noise and hum pickup. The d-c supply for the heaters of the low-level tubes should be made integral to the reproducer unit. There should be tape guides near both the take-up and pay-out reels to fix more definitely the position of the tape on the reels. There should be a vertical adjustment on the band assembly to maximize the response without forcing the tape out of its natural path. Investigations should be made into the procurement of a more flexible magnetic tape that is less subject to humidity effects.

REFERENCES

1. Greenhouse Report WT-107(Ref.), Annex 1.2, Part I, Sec. 8.1.1.
2. Greenhouse Report WT-107(Ref.), Annex 1.2, Part I, Sec. 4.5.
3. Greenhouse Report WT-107(Ref.), Annex 1.2, Part I, Fig. 3.8.
4. Greenhouse Report WT-41, Annex 1.2, Part IV.
5. L. D. P. King and F. L. Bentzen, Gamma-ray Intensities at the Sandstone Tests in the Region 0-1000 Microseconds, Los Alamos Scientific Laboratory Report, LAB-J-539 (not available).
6. Greenhouse Report WT-107(Ref.), Annex 1.2, Part I, Chap. III.
7. Greenhouse Report wT-107(Ref.), Annex 1.2, Part I, Chap. V.
8. Greenhouse Report WT-107(Ref.), Annex 1.2, Part I, Chap. VI.
9. Greenhouse Report WT-77, Annex 1.2, Part II, Fig. 6.1.
10. Greenhouse Report WT-107(Ref.), Annex 1.2, Part I, Appendix A.
11. W. V. Mayneord, Some Applications of Nuclear Physics to Medicine, Brit. J. Radiol., Suppl. 2: 136 (1950).
12. L. Costrell, National Bureau of Standards, Work on Operation Jangle.